Optical Properties of Solids

MARK FOX

Department of Physics and Astronomy
University of Sheffield

OXFORD
UNIVERSITY PRESS

OXFORD
UNIVERSITY PRESS
Great Clarendon Street, Oxford OX2 6DP

Oxford University Press is a department of the University of Oxford.
It furthers the University's objective of excellence in research, scholarship,
and education by publishing worldwide in

Oxford New York

Auckland Cape Town Dar es Salaam Hong Kong Karachi
Kuala Lumpur Madrid Melbourne Mexico City Nairobi
New Delhi Shanghai Taipei Toronto

With offices in

Argentina Austria Brazil Chile Czech Republic France Greece
Guatemala Hungary Italy Japan Poland Portugal Singapore
South Korea Switzerland Thailand Turkey Ukraine Vietnam

Oxford is a registered trade mark of Oxford University Press
in the UK and in certain other countries

Published in the United States
by Oxford University Press Inc., New York

© Oxford University press, 2001

The moral rights of the author have been asserted
Database right Oxford University Press (maker)

First published 2001
Reprinted 2003 (with corrections), 2004, 2005, 2006, 2007 (with corrections)

All rights reserved. No part of this publication may be reproduced,
stored in a retrieval system, or transmitted, in any form or by any means,
without the prior permission in writing of Oxford University Press,
or as expressly permitted by law, or under terms agreed with the appropriate
reprographics rights organization. Enquiries concerning reproduction
outside the scope of the above should be sent to the Rights Department,
Oxford University Press, at the address above

You must not circulate this book in any other binding or cover
and you must impose the same condition on any acquirer

British Library Cataloguing in Publication Data

Data available

Library of Congress Cataloging in Publication Data

Fox, Mark (Anthony Mark)
  Optical properties of solids / Mark Fox.
    p. cm. — (Oxford master series in condensed matter physics)
  Includes index.
  1. Solids—Optical properties. I. Title. II. Series.

QC176.8 O6 F69 2001 530.4'12—dc21 2001036967

Printed in Great Britain
on acid-free paper by
Antony Rowe Ltd., Chippenham, Wiltshire

ISBN 978-0-19-850613-3 (hardback)
ISBN 978-0-19-850612-6 (paperback)

10 9 8 7 6

Introduction

1

Light interacts with matter in many different ways. Metals are shiny, but water is transparent. Stained glass and gemstones transmit some colours, but absorb others. Other materials such as milk appear white because they scatter the incoming light in all directions.

In the chapters that follow, we will be looking at a whole host of these optical phenomena in a wide range of solid state materials. Before we can begin to do this, we must first describe the way in which the phenomena are classified, and the coefficients that are used to quantify them. We must then introduce the materials that we will be studying, and clarify in general terms how the solid state is different from the gas and liquid phase. This is the subject of the present chapter.

1.1 Classification of optical processes

The wide-ranging optical properties observed in solid state materials can be classified into a small number of general phenomena. The simplest group, namely **reflection**, **propagation** and **transmission**, is illustrated in Fig. 1.1. This shows a light beam incident on an optical medium. Some of the light is reflected from the front surface, while the rest enters the medium and propagates through it. If any of this light reaches the back surface, it can be reflected again, or it can be transmitted through to the other side. The amount of light transmitted is therefore related to the reflectivity at the front and back surfaces and also to the way the light propagates through the medium.

The phenomena that can occur while light propagates through an optical medium are illustrated schematically in Fig. 1.2.

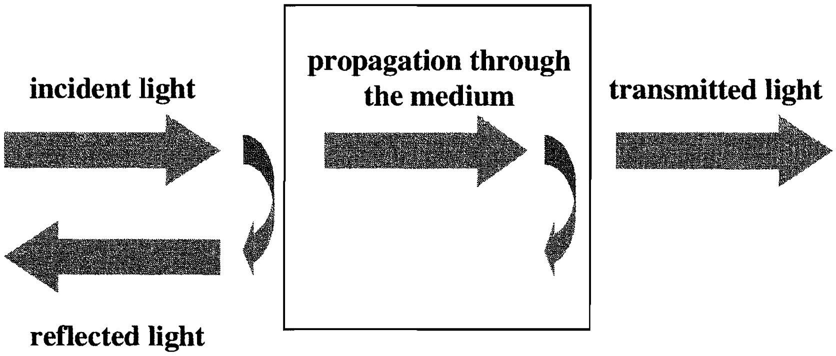

Fig. 1.1 Reflection, propagation and transmission of a light beam incident on an optical medium.

Refraction causes the light waves to propagate with a smaller velocity than in free space. This reduction of the velocity leads to the bending of light rays at interfaces described by Snell's law of refraction. Refraction, in itself, does not affect the intensity of the light wave as it propagates.

Absorption occurs during the propagation if the frequency of the light is resonant with the transition frequencies of the atoms in the medium. In this case, the beam will be attenuated as it progresses. The transmission of the medium is clearly related to the absorption, because only unabsorbed light will be transmitted. Selective absorption is responsible for the colouration of many optical materials. Rubies, for example, are red because they absorb blue and green light, but not red.

Luminescence is the general name given to the process of spontaneous emission of light by excited atoms in a solid state material. One of the ways in which the atoms can be promoted into excited states prior to spontaneous emission is by the absorption of light. Luminescence can thus accompany the propagation of light in an absorbing medium. The light is emitted in all directions, and has a different frequency to the incoming beam.

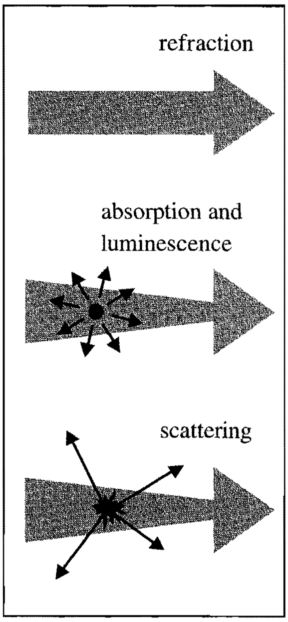

Fig. 1.2 Phenomena that can occur as a light beam propagates through an optical medium. Refraction causes a reduction in the velocity of the wave, while absorption causes attenuation. Luminescence can accompany absorption if the excited atoms re-emit by spontaneous emission. Scattering causes a redirection of the light. The diminishing width of the arrow for the processes of absorption and scattering represents the attenuation of the beam.

Luminescence does not always have to accompany absorption. It takes a characteristic amount of time for the excited atoms to re-emit by spontaneous emission. This means that it might be possible for the excited atoms to dissipate the excitation energy as heat before the radiative re-emission process occurs. The efficiency of the luminescence process is therefore closely tied up with the dynamics of the de-excitation mechanisms in the atoms.

Scattering is the phenomenon in which the light changes direction and possibly also its frequency after interacting with the medium. The total number of photons is unchanged, but the number going in the forward direction decreases because light is being re-directed in other directions. Scattering therefore has the same attenuating effect as absorption. The scattering is said to be **elastic** if the frequency of the scattered light is unchanged, or **inelastic** if the frequency changes in the process. The difference in the photon energy in an inelastic scattering process has to be taken from the medium if the frequency increases or given to the medium if the frequency decreases.

A number of other phenomena can occur as the light propagates through the medium if the intensity of the beam is very high. These are described by **nonlinear optics**. An example is frequency doubling, in which the frequency of part of a beam is doubled by interaction with the optical medium. These nonlinear effects have only been discovered through the use of lasers. At this stage, we only mention their existence for completeness, and postpone their further discussion until Chapter 11.

1.2 Optical coefficients

The optical phenomena described in the previous section can be quantified by a number of parameters that determine the properties of the medium at the macroscopic level.

The reflection at the surfaces is described by the **coefficient of reflection** or **reflectivity**. This is usually given the symbol R and is defined as the ratio of the reflected power to the power incident on the surface. The **coefficient**

of transmission or **transmissivity** T is defined likewise as the ratio of the transmitted power to the incident power. If there is no absorption or scattering, then by conservation of energy we must have that:

$$R + T = 1\,. \tag{1.1}$$

The propagation of the beam through a transparent medium is described by the **refractive index** n. This is defined as the ratio of the velocity of light in free space c to the velocity of light in the medium v according to:

$$n = \frac{c}{v}\,. \tag{1.2}$$

The refractive index depends on the frequency of the light beam. This effect is called **dispersion**, and will be discussed in detail in Section 2.3. In colourless transparent materials such as glass, the dispersion is small in the visible spectral region, and it therefore makes sense to speak of 'the' refractive index of the substance in question.

The absorption of light by an optical medium is quantified by its **absorption coefficient** α. This is defined as the fraction of the power absorbed in a unit length of the medium. If the beam is propagating in the z direction, and the intensity (optical power per unit area) at position z is $I(z)$, then the decrease of the intensity in an incremental slice of thickness dz is given by:

$$dI = -\alpha dz \times I(z)\,. \tag{1.3}$$

This can be integrated to obtain **Beer's law**:

$$I(z) = I_0 \mathrm{e}^{-\alpha z}\,, \tag{1.4}$$

where I_0 is the optical intensity at $z = 0$. The absorption coefficient is a strong function of frequency, so that optical materials may absorb one colour but not another.

In the next section we will explain how both the absorption and the refraction can be incorporated into a single quantity called the complex refractive index. Knowledge of this quantity enables us to calculate the reflectivity R, and hence the transmissivity T. This last point follows because the transmissivity of an absorbing medium of thickness l is given by:

$$T = (1 - R_1)\,\mathrm{e}^{-\alpha l}\,(1 - R_2)\,, \tag{1.5}$$

where R_1 and R_2 are the reflectivities of the front and back surfaces respectively. This formula applies to the transmission of light through an optical medium such as the one shown in Fig. 1.1. The first and third terms on the right hand side of eqn 1.5 account for the transmission of the front and back surfaces respectively, while the middle term gives the exponential decrease in intensity due to the absorption according to Beer's law. If the front and back surfaces have equal reflectivities R, as will usually be the case, then eqn 1.5 simplifies to:

$$T = (1 - R)^2\,\mathrm{e}^{-\alpha l}\,. \tag{1.6}$$

Equation (1.5) ignores the possibility of multiple reflections between the front and back surfaces. These will have to be included if the surfaces are parallel and the reflection coefficients are sufficiently large. We will come across some examples where these effects are important when we consider semiconductor laser diodes in Section 5.4.3 and optical bistability in Section 11.4.3. In many cases, however, the effects are small enough to be neglected, as shown in Exercises 1.8 and 1.9.

The optical density, and hence the absorption coefficient, is usually worked out from the measured transmissivity of the sample. This requires accurate normalization of the reflection losses at the surfaces. (See Exercise 1.10.)

The absorption of an optical medium can also be sometimes quantified in terms of the **optical density** (O.D.). This is sometimes called the **absorbance**, and is defined as:

$$\text{O.D.} = -\log_{10}\left(\frac{I(l)}{I_0}\right), \tag{1.7}$$

where l is the length of the absorbing medium. It is apparent from eqn 1.4 that the optical density is directly related to the absorption coefficient α through:

$$\text{O.D.} = \frac{\alpha l}{\log_e(10)} = 0.434\,\alpha l\,. \tag{1.8}$$

In this book we will quantify the absorption by α instead of the optical density because it is independent of the sample length.

The phenomenon of luminescence was studied extensively by George Stokes in the nineteenth century before the advent of quantum theory. Stokes discovered that the luminescence is down-shifted in frequency relative to the absorption, an effect now known as the **Stokes shift**. Luminescence cannot be described easily by macroscopic classical parameters because spontaneous emission is fundamentally a quantum process (see Appendix B).

The simplest sequence of events that takes place in luminescence is illustrated in Fig. 1.3. The atom jumps to an excited state by absorbing a photon, then relaxes to an intermediate state, and finally re-emits a photon as it drops back to the ground state. The Stokes shift is explained by applying the law of conservation of energy to the process. It is easy to see that the energy of the photon emitted must be less than that of the photon absorbed, and hence that the frequency of the emitted light is less than that of the absorbed light. The magnitude of the Stokes shift is therefore determined by the energy levels of the atoms in the medium.

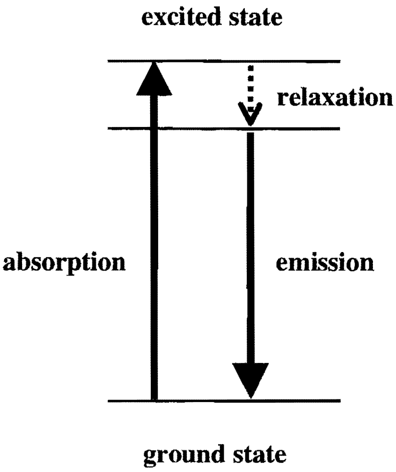

Fig. 1.3 Luminescence process in an atom. The atom jumps to an excited state by absorption of a photon, then relaxes to an intermediate state, before re-emitting a photon by spontaneous emission as it falls back to the ground state. The photon emitted has a smaller energy than the absorbed photon. This reduction in the photon energy is called the Stokes shift.

Scattering is caused by variations of the refractive index of the medium on a length scale smaller than the wavelength of the light. This could be caused by the presence of impurities, defects, or inhomogeneities. Scattering causes attenuation of a light beam in an analogous way to absorption. The intensity decreases exponentially as it propagates into the medium according to:

$$I(z) = I_0 \exp(-N\sigma_s z)\,, \tag{1.9}$$

where N is the number of scattering centres per unit volume, and σ_s is the **scattering cross-section** of the scattering centre. This is identical in form to Beer's law given in eqn 1.4, with $\alpha \equiv N\sigma_s$.

The scattering is described as **Rayleigh scattering** if the size of the scattering centre is very much smaller than the wavelength of the light. In this case, the scattering cross-section will vary with the wavelength λ according to:

$$\sigma_s(\lambda) \propto \frac{1}{\lambda^4}\,. \tag{1.10}$$

The Rayleigh scattering law implies that inhomogeneous materials tend to scatter short wavelengths more strongly than longer wavelengths.

Example 1.1

The reflectivity of silicon at 633 nm is 35% and the absorption coefficient is $3.8 \times 10^5\ \mathrm{m}^{-1}$. Calculate the transmission and optical density of a sample with a thickness of 10 μm.

Solution

The transmission is given by eqn 1.6 with $R = 0.35$ and $\alpha l = (3.8 \times 10^5) \times (10 \times 10^{-6}) = 3.8$. This gives:

$$T = (1 - 0.35)^2 \cdot \exp(-3.8) = 0.0095\,.$$

The optical density is given by eqn 1.8:

$$\mathrm{O.D.} = 0.434 \times 3.8 = 1.65\,.$$

1.3 The complex refractive index and dielectric constant

In the previous section we mentioned that the absorption and refraction of a medium can be described by a single quantity called the **complex refractive index**. This is usually given the symbol $\tilde{n}$ and is defined through the equation:

$$\tilde{n} = n + i\kappa\,. \tag{1.11}$$

The real part of $\tilde{n}$, namely n, is the same as the normal refractive index defined in eqn. 1.2. The imaginary part of $\tilde{n}$, namely κ, is called the **extinction coefficient**. As we will see below, κ is directly related to the absorption coefficient α of the medium.

The relationship between α and κ can be derived by considering the propagation of plane electromagnetic waves through a medium with a complex refractive index. If the wave is propagating in the z direction, the spatial and time dependence of the electric field is given by (see eqn A.32 in Appendix A):

$$\mathcal{E}(z,t) = \mathcal{E}_0\, \mathrm{e}^{i(kz-\omega t)}\,, \tag{1.12}$$

where k is the wave vector of the light and ω is the angular frequency. $|\mathcal{E}_0|$ is the amplitude at $z = 0$. In a non-absorbing medium of refractive index n, the wavelength of the light is reduced by a factor n compared to the free space wavelength λ. k and ω are therefore related to each other through:

$$k = \frac{2\pi}{(\lambda/n)} = \frac{n\omega}{c}\,. \tag{1.13}$$

This can be generalized to the case of an absorbing medium by allowing the refractive index to be complex:

$$k = \tilde{n}\frac{\omega}{c} = (n + i\kappa)\frac{\omega}{c}\,. \tag{1.14}$$

On substituting eqn 1.14 into eqn 1.12, we obtain:

$$\begin{aligned}\mathcal{E}(z,t) &= \mathcal{E}_0\, \mathrm{e}^{i(\omega\tilde{n}z/c-\omega t)} \\ &= \mathcal{E}_0\, \mathrm{e}^{-\kappa\omega z/c}\, \mathrm{e}^{i(\omega n z/c-\omega t)}\,. \end{aligned} \tag{1.15}$$

This shows that a non-zero extinction coefficient leads to an exponential decay of the wave in the medium. At the same time, the real part of $\tilde{n}$ still determines the phase velocity of the wave front, as in the standard definition of the refractive index given in eqn 1.2.

The optical intensity of a light wave is proportional to the square of the electric field, namely $I \propto \mathcal{E}\mathcal{E}^*$ (c.f. eqn A.40). We can therefore deduce from eqn 1.15 that the intensity falls off exponentially in the medium with a decay constant equal to $2 \times (\kappa\omega/c)$. On comparing this to Beer's law given in eqn 1.4 we conclude that:

$$\alpha = \frac{2\kappa\omega}{c} = \frac{4\pi\kappa}{\lambda}\,, \tag{1.16}$$

where λ is the free space wavelength of the light. This shows us that κ is directly proportional to the absorption coefficient.

We can relate the refractive index of a medium to its relative dielectric constant ϵ_r by using the standard result derived from Maxwell's equations (cf. eqn A.31 in Appendix A):

$$n = \sqrt{\epsilon_\mathrm{r}}\,. \tag{1.17}$$

This shows us that if n is complex, then ϵ_r must also be complex. We therefore define the **complex relative dielectric constant** $\tilde{\epsilon}_\mathrm{r}$ according to:

$$\tilde{\epsilon}_\mathrm{r} = \epsilon_1 + i\epsilon_2\,. \tag{1.18}$$

By analogy with eqn 1.17, we see that $\tilde{n}$ and $\tilde{\epsilon}_\mathrm{r}$ are related to each other through:

$$\tilde{n}^2 = \tilde{\epsilon}_\mathrm{r} \tag{1.19}$$

We can now work out explicit relationships between the real and imaginary parts of $\tilde{n}$ and $\tilde{\epsilon}_\mathrm{r}$ by combining eqns 1.11, 1.18 and 1.19. These are:

$$\epsilon_1 = n^2 - \kappa^2 \tag{1.20}$$

$$\epsilon_2 = 2n\kappa\,, \tag{1.21}$$

and

$$n = \frac{1}{\sqrt{2}}\left(\epsilon_1 + (\epsilon_1^2+\epsilon_2^2)^{\frac{1}{2}}\right)^{\frac{1}{2}} \tag{1.22}$$

$$\kappa = \frac{1}{\sqrt{2}}\left(-\epsilon_1 + (\epsilon_1^2+\epsilon_2^2)^{\frac{1}{2}}\right)^{\frac{1}{2}}\,. \tag{1.23}$$

This analysis shows us that $\tilde{n}$ and $\tilde{\epsilon}_\mathrm{r}$ are not independent variables: if we know ϵ_1 and ϵ_2 we can calculate n and κ, and *vice versa*. Note that if the medium is only weakly absorbing, then we can assume that κ is very small, so that eqns 1.22 and 1.23 simplify to:

$$n = \sqrt{\epsilon_1} \tag{1.24}$$

$$\kappa = \frac{\epsilon_2}{2n}\,. \tag{1.25}$$

These equations show us that the refractive index is basically determined by the real part of the dielectric constant, while the absorption is mainly determined by the imaginary part. This generalization is obviously not valid if the medium has a very large absorption coefficient.

The microscopic models that we will be developing throughout the book usually enable us to calculate $\tilde{\epsilon}_r$ rather than $\tilde{n}$. The measurable optical properties can then be obtained by converting ϵ_1 and ϵ_2 to n and κ through eqns 1.22 and 1.23. The refractive index is given directly by n, while the absorption coefficient can be worked out from κ using eqn 1.16. The reflectivity depends on both n and κ and is given by

$$R = \left| \frac{\tilde{n} - 1}{\tilde{n} + 1} \right|^2 = \frac{(n-1)^2 + \kappa^2}{(n+1)^2 + \kappa^2} . \tag{1.26}$$

This formula is derived in eqn A.50. It gives the coefficient of reflection between the medium and the air (or vacuum) at normal incidence.

In a transparent material such as glass in the visible region of the spectrum, the absorption coefficient is very small. Equations 1.16 and 1.21 then tell us that κ and ϵ_2 are negligible, and hence that both $\tilde{n}$ and $\tilde{\epsilon}_r$ may be taken as real numbers. This is why tables of the properties of transparent optical materials generally list only the real parts of the refractive index and dielectric constant. On the other hand, if there is significant absorption, then we will need to know both the real and imaginary parts of $\tilde{n}$ and $\tilde{\epsilon}_r$.

In the remainder of this book we will take it as explicitly assumed that both the refractive index and the dielectric constant are complex quantities. We will therefore drop the tilde notation on n and ϵ_r from now on, except where it is explicitly needed to avoid ambiguity. It will usually be obvious from the context whether we are dealing with real or complex quantities.

Example 1.2

The complex refractive index of germanium at 400 nm is given by $\tilde{n} = 4.141 + i\,2.215$. Calculate for germanium at 400 nm: (a) the phase velocity of light, (b) the absorption coefficient, and (c) the reflectivity.

Solution

(a) The velocity of light is given by eqn 1.2, where n is the real part of $\tilde{n}$. Hence we obtain:

$$v = \frac{c}{n} = \frac{2.998 \times 10^8}{4.141}\,\mathrm{m\,s^{-1}} = 7.24 \times 10^7\,\mathrm{m\,s^{-1}} .$$

(b) The absorption coefficient is given by eqn 1.16. By inserting $\kappa = 2.215$ and $\lambda = 400\,\mathrm{nm}$, we obtain:

$$\alpha = \frac{4\pi \times 2.215}{400 \times 10^{-9}}\,\mathrm{m^{-1}} = 6.96 \times 10^7\,\mathrm{m^{-1}} .$$

(c) The reflectivity is given by eqn 1.26. Inserting $n = 4.141$ and $\kappa = 2.215$ into this, we obtain:

$$R = \frac{(4.141 - 1)^2 + 2.215^2}{(4.141 + 1)^2 + 2.215^2} = 47.1\,\% .$$

Example 1.3

We will see in Chapter 10 that the restrahlen absorption is caused by the interaction between the light and the optical phonons.

Salt (NaCl) absorbs very strongly at infrared wavelengths in the 'restrahlen' band. The complex dielectric constant at 60 μm is given by $\tilde{\epsilon}_r = -16.8 + i\,91.4$. Calculate the absorption coefficient and the reflectivity at this wavelength.

Solution

We must first work out the complex refractive index using eqns 1.22 and 1.23. This gives:

$$n = \frac{1}{\sqrt{2}}\left(-16.8 + ((-16.8)^2 + 91.4^2)^{\frac{1}{2}}\right)^{\frac{1}{2}} = 6.17$$

and

$$\kappa = \frac{1}{\sqrt{2}}\left(+16.8 + ((-16.8)^2 + 91.4^2)^{\frac{1}{2}}\right)^{\frac{1}{2}} = 7.41\,.$$

We then insert these values into eqns 1.16 and 1.26 to obtain the required results:

$$\alpha = \frac{4\pi \times 7.41}{60 \times 10^{-6}}\ \mathrm{m}^{-1} = 1.55 \times 10^{6}\ \mathrm{m}^{-1}\,,$$

and

$$R = \frac{(6.17-1)^2 + 7.41^2}{(6.17+1)^2 + 7.41^2} = 76.8\ \%\,.$$

1.4 Optical materials

We will be studying the optical properties of many different types of solid state materials throughout this book. The materials can be loosely classified into five general categories:

- Crystalline insulators and semiconductors
- Glasses
- Metals
- Molecular materials
- Doped glasses and insulators.

Before delving into the details, we give here a brief overview of the main optical properties of these materials. This will serve as an introduction to the optical physics that will be covered in the following chapters.

1.4.1 Crystalline insulators and semiconductors

Figure 1.4(a) shows the transmission spectrum of crystalline sapphire (Al_2O_3) from the infrared to the ultraviolet spectral region. The spectrum for sapphire shows the main features observed in all insulators, although of course the details will vary considerably from material to material. The principal optical properties can be summarized as follows:

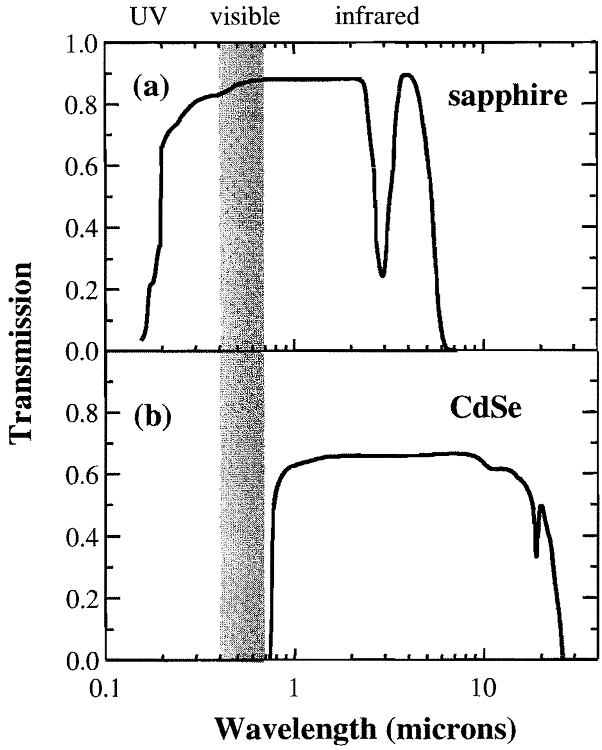

Fig. 1.4 (a) Transmission spectrum of a sapphire (Al_2O_3) crystal of thickness 3 mm. (b) Transmission spectrum of a CdSe crystal of thickness 1.67 mm. After [1].

(1) Sapphire has a high transmission in the wavelength range 0.2–6 μm. This defines the **transparency range** of the crystal. The transparency region of sapphire includes the whole of the visible spectrum, which explains why it appears colourless and transparent to the human eye.

(2) Within the transparency range the absorption coefficient is very small, and the refractive index may be taken to be real with no imaginary component. The value of the refractive index is approximately constant, and is equal to 1.77 in sapphire.

Sapphire gemstones tend to be blue. This is caused by the presence of chromium, titanium and iron impurities in the Al_2O_3 crystal. Pure synthetic Al_2O_3 crystals are colourless.

(3) The transmission coefficient in the transparency range is determined by the reflectivity of the surfaces through eqn 1.6. The reflectivity in turn is determined by the refractive index through eqn 1.26. For sapphire with $n = 1.77$, this gives $R = 0.077$. Hence we find $T = (1 - R)^2 = 0.85$.

(4) The dip in the transmission in the infrared around 3 μm, and the sharp drop in the transmission for $\lambda > 6\,\mu$m, is caused by vibrational absorption. This absorption mechanism is analogous to the infrared absorption due to vibrations in polar molecules. The vibrational excitations of a crystal lattice are called phonon modes, and so the vibrational absorption in a solid is usually called phonon absorption or lattice absorption. This absorption mechanism will be discussed in Chapter 10.

Sapphire actually transmits in the far infrared spectral region when the frequency is well below that of the optical phonons.

(5) The transmission drops sharply in the ultraviolet spectral region for $\lambda < 0.2\,\mu$m due to absorption by bound electrons. The onset of the absorption is called the **fundamental absorption edge**. The wavelength of the fundamental edge is determined by the band gap of the insulator. The

explanation of the absorption spectra due to bound electrons needs band theory, and will be discussed in Chapters 3 and 4.

Point (1) is perhaps the most obvious aspect of the optical properties of insulators: they all tend to be colourless and transparent in the visible spectral region. If they are coloured, this is most likely caused by the presence of impurities, as will be explained in Section 1.4.5 below. This transparency is slightly deceptive. The insulators do absorb very strongly in the ultraviolet and in the infrared, but this is hidden from the human eye. The transparent region between the infrared and ultraviolet absorption bands is particularly useful for making optical windows and lenses. The approximate transparency range and refractive index of a number of common crystalline insulators are listed in Table 1.1.

The very high transparency of diamond in the infrared is noteworthy. This is caused by the fact that diamond is a purely covalent crystal, which means that its optical phonons cannot interact directly with light waves. This point will be discussed further in Chapter 10.

Table 1.1 Approximate transparency range and refractive index n of a number of crystalline insulators. n is measured at 546 nm. Values of n are given both for the o-ray and e-ray of birefringent materials. After [1] and [2].

Crystal	Transparency range (μm)	n
Al_2O_3 (sapphire)	0.2–6	1.771 (o) 1.763 (e)
BaF_2	0.2–12	1.476
Diamond	0.25–> 80	2.424
KBr	0.3–30	1.564
KCl	0.21–25	1.493
KI	0.3–40	1.673
MgF_2	0.12–8	1.379 (o) 1.390 (e)
NaCl	0.21–20	1.55
NaF	0.19–15	1.326
SiO_2 (quartz)	0.2–3	1.546 (o) 1.555 (e)
TiO_2 (rutile)	0.45–5	2.652 (o) 2.958 (e)

The crystallinity of the materials gives rise to a number of properties relating to the underlying symmetry of the lattice. This point will be expanded further in Section 1.5.1. One immediate consequence is that some of the materials listed in Table 1.1 are birefringent. The optical properties are anisotropic, and the value of the refractive index depends on the direction of propagation of the light relative to the crystallographic axes. The phenomenon of birefringence will be described in more detail in Section 2.4.

The optical properties of semiconductors are conceptually similar to those of insulators, except that the electronic and vibrational transitions occur at longer wavelengths. By way of example, Fig. 1.4(b) shows the transmission spectrum of the II–VI compound semiconductor CdSe over the same wavelength range as for the sapphire crystal. Just as with sapphire, we have a transparency range which is limited by electronic absorption at short wavelengths and lattice absorption at long wavelengths. The maximum transmission is around 60% which is again mainly limited by the surface reflectivities. The short wavelength edge occurs beyond 700 nm, which means that the whole of the transparency range lies outside the visible spectrum. Hence no visible light is transmitted through the crystal, and it has a dark metallic appearance to the eye.

Table 1.2 lists the transparency range and refractive index of several semiconductors. The data show that the lower limit of the transmission range coincides closely with the wavelength of the fundamental band gap. This happens because the band gap determines the lowest energy for interband transitions, as will be explained in Chapter 3. Note that the refractive index increases as the band gap wavelength gets larger.

The upper limit of the transmission range is determined by the lattice absorption, as for insulators, and also by free carrier absorption. Free carriers are present in semiconductors at room temperature through the thermal excitation of electrons across the band gap or due to the presence of impurities. This causes infrared absorption, as will be explained in Section 7.4. Insulators have very small free carrier densities due to their large band gaps.

One very important aspect of the optical properties of semiconductors is that a subset of them, namely those with direct band gaps, luminesce strongly when electrons are promoted to the conduction band. This is the physical basis for the light-emitting devices used in the optoelectronics industry. The physical processes behind the luminescence will be explained in Chapter 5. The main point is that the wavelength of the luminescence coincides with the band gap of the semiconductor. In Chapter 6 we will see how quantum size effects in low-dimensional semiconductors can be used to shift the effective band gap to higher energy. This is a highly desirable feature, because it provides a way to 'tune' the emission wavelength by controlled variation of the parameters during the crystal growth.

Table 1.2 Approximate transparency range, band gap wavelength λ_g, and refractive index n of a number of common semiconductors. n is measured at 10 μm. After [1], [2] and [3].

Crystal	Transparency range (μm)	λ_g (μm)	n
Ge	1.8–23	1.8	4.00
Si	1.2–15	1.1	3.42
GaAs	1.0–20	0.87	3.16
CdTe	0.9–14	0.83	2.67
CdSe	0.75–24	0.71	2.50
ZnSe	0.45–20	0.44	2.41
ZnS	0.4–14	0.33	2.20

1.4.2 Glasses

Glasses are extremely important optical materials. They have been used for centuries in prisms and lenses for optical instruments, in addition to their common usage in windows and glassware. In more recent times they have found new applications in optical fibre technology. With the exception of stained glasses, they are usually made to be transparent in the visible spectrum. They are not crystalline solids, and therefore do not exhibit the optical anisotropy that is characteristic of some crystals.

Most types of glasses are made by fusing sand (silica: SiO_2) with other chemicals. Pure fused silica is an insulator, and shows all the characteristic features of insulators discussed in the previous section. It is transparent in the visible region, but absorbs in the ultraviolet due to the electronic transitions of the SiO_2 molecules, and in the infrared due to vibrational absorption. The transparency range thus goes from around 200 nm in the ultraviolet to beyond 2000 nm in the infrared.

The properties of fused silica will be described in more detail in Section 2.2.3. Fused silica is used extensively in the fibre optics industry, as the principal material from which many fibres are made. It has been refined to such an extent that the absorption and scattering losses are so small that light can travel many kilometres down the fibre before being fully attenuated.

The refractive index of silica in the transparency range is tabulated against the wavelength in Table 1.3. This variation of the refractive index with wavelength is called dispersion. Note that it is not a very large effect: n changes by less than 1 % over the whole visible spectral region. Note also that the dispersion is largest at the shortest wavelengths near the fundamental absorption edge. Dispersion is present in all optical materials, as will be explained in Section 2.3.

Table 1.3 Refractive index of synthetic fused silica versus wavelength. After [2].

Wavelength (nm)	Refractive index
213.9	1.53430
239.9	1.51336
275.3	1.49591
334.2	1.47977
404.7	1.46962
467.8	1.46429
508.6	1.46186
546.1	1.46008
632.8	1.45702
706.5	1.45515
780.0	1.45367
1060	1.44968
1395	1.44583
1530	1.44427
1970	1.43853
2325	1.43293

Chemicals are commonly added to silica during the fusion process to produce a whole range of other types of glasses. The presence of these additives can alter the refractive index and the transmission range. Table 1.4.2 lists the composition of a number of common glasses together with their refractive index and ultraviolet transmission. It is apparent that the additives have the effect of increasing the refractive index, at the expense of increasing the ultraviolet absorption. A high refractive index is desirable for cut-glass products, since it increases the reflectivity (see Exercise 1.2), and hence gives the glassware a more shiny appearance.

Stained glass and colour glass filters are made by adding semiconductors with band gaps in the visible spectral region during the fusion process. The properties of these coloured glasses will be discussed further in Section 1.4.5 below.

Table 1.4 Composition, refractive index and ultraviolet transmission of common glasses. The letters after the names give the abbreviations used to identify the glass type. The composition figures are the percentage by mass. The refractive index is measured at 546.1 nm, and the transmission is for a 1 cm plate at 310 nm. After [1], [4].

Name	SiO_2	B_2O_3	Al_2O_3	Na_2O	K_2O	CaO	BaO	PbO	P_2O_5	*n*	*T*
Fused silica	100									1.460	0.91
Crown (K)	74			9	11	6				1.513	0.4
Borosilicate crown (BK)	70	10		8	8	1	3			1.519	0.35
Phosphate crown (PK)		3	10		12	5			70	1.527	0.46
Light flint (LF)	53			5	8			34		1.585	0.008
Flint (F)	47			2	7			44		1.607	–
Dense flint (SF)	33				5			62		1.746	–

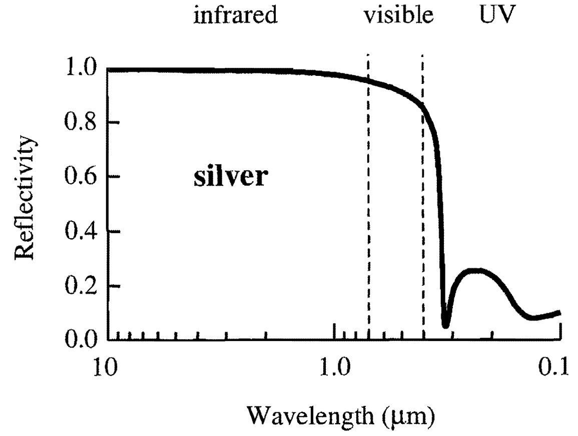

Fig. 1.5 Reflectivity of silver from the infrared to the ultraviolet. After [4].

1.4.3 Metals

The characteristic optical feature of metals is that they are shiny. This is why metals like silver and aluminium have been used for making mirrors for centuries. The shiny appearance is a consequence of their very high reflection coefficients. We will see in Chapter 7 that the high reflectivity is caused by the interaction of the light with the free electrons that are present in the metal.

Figure 1.5 shows the reflectivity of silver from the infrared spectral region to the ultraviolet. We see that the reflectivity is very close to 100 % in the infrared, and stays above 80 % throughout the whole visible spectral region. The reflectivity then drops sharply in the ultraviolet. This general behaviour is observed in all metals. There is strong reflection for all frequencies below a characteristic cut-off frequency called the plasma frequency. The plasma frequency corresponds to a wavelength in the ultraviolet spectral region, and so metals reflect infrared and visible wavelengths, but transmit ultraviolet wavelengths. This effect is called the ultraviolet transmission of metals.

Some metals have characteristic colours. Copper, for example, has a pinkish colour, while gold is yellowish. These colours are caused by interband electronic transitions that occur in addition to the free carrier effects that cause the reflection. This point will be explained in Section 7.3.2 of Chapter 7.

1.4.4 Molecular materials

The term 'molecular material' could in principle cover the solid phase of any molecule. However, the crystalline phase of inorganic molecules such as NaCl or GaAs are classified as insulators or semiconductors in this book, while simple organic molecules such as methane (CH_4) tend to be gases or liquids at room temperature. We therefore restrict our attention here to large organic molecules.

Some organic compounds form crystals in the condensed phase, but many others are amorphous. The solids are held together by the relatively weak van der Waals interactions between the molecules, which are themselves held together by strong covalent bonds. The optical properties of the solid therefore tend to be very similar to those of the individual molecules.

Organic compounds can be generally classified into either saturated or conjugated systems. This classification depends on the type of bonding in the molecule, and will be explained in more detail in Chapter 8.

In saturated compounds, the valence electrons are incorporated into strong, localized bonds between neighbouring atoms. This means that all the electrons are tightly held in their bonds, and can only respond at high frequencies in the ultraviolet spectral range. Saturated compounds are therefore usually colourless and do not absorb in the visible region. Their properties are generally similar to those of the glasses discussed in Section 1.4.2 above; they absorb in the infrared and ultraviolet due to vibrational and electronic transitions respectively, and are transparent in the visible. Plastics such as poly-methyl-methacrylate (commonly known as 'perspex' or 'plexiglass') or poly-ethylene (polythene) are typical examples.

Conjugated molecules, by contrast, have much more interesting optical properties. The electrons from the p-like atomic states of the carbon atoms form large delocalized orbitals called π orbitals which spread out across the whole molecule. The standard example of a conjugated molecule is benzene (C_6H_6), in which the π electrons form a ring-like orbital above and below the plane of the carbon and hydrogen atoms. Further examples include the other aromatic hydrocarbons, dye molecules, and conjugated polymers.

π electrons are less tightly bound than the electrons in saturated molecules, and are optically-active at lower frequencies. In benzene the absorption edge is in the ultraviolet at 260 nm, but with other molecules the transition energy is shifted down to visible frequencies. The molecules with visible absorption also tend to emit strongly at visible frequencies. This makes them of high technological interest for applications as light-emitting devices. These are the solid state counterparts of the organic dyes that have been used in liquid lasers for several decades.

The optical processes that occur in π conjugated materials will be described in Chapter 8. By way of example, Fig. 1.6 shows the absorption spectrum of the technologically important polyfluorene-based polymer called 'F8'. Thin film samples of this material are typically prepared by spin coating the molecules onto a glass slide. The data in Fig. 1.6 show that the polymer is transparent throughout most of the visible spectral region, but absorbs strongly at ultraviolet wavelengths. The broad absorption band which peaks at 380 nm is caused by vibrational–electronic transitions to the first singlet excited state of the

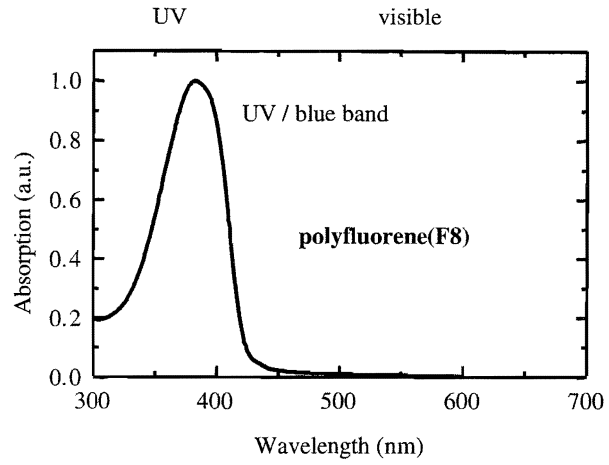

Fig. 1.6 Absorption spectrum of the polyfluorene-based polymer F8 [poly(9,9-dioctylfluorene)]. After [5], copyright 2001 Exerpta Medica Inc., reprinted with permission.

molecule. This band extends slightly into the blue spectral region, and gives the material a pale yellow colour.

Conjugated polymers such as F8 luminesce strongly when electrons are promoted into the excited states of the molecule. The luminescence is Stokes shifted to lower energy compared to the absorption, and typically occurs in the middle of the visible spectral region. An attractive feature of these organic materials is that the emission wavelength can be 'tuned' by small alterations to the chemical structure of the molecular units within the polymers. We will see in Section 8.6 how this property has been used to develop organic light-emitting devices to cover the full range of the visible spectral region.

1.4.5 Doped glasses and insulators

We have already mentioned in Section 1.4.2 above that colour glass filters and stained glass are made by adding appropriately chosen semiconductors to silica during the fusion process. This is a typical example of how a colourless material such as fused silica can take on new properties by controlled doping with optically active substances.

The colour of a colour glass filter can be controlled in two different ways.

(1) The most obvious way is by variation of the composition of the dopant. For example, the glass might be doped with the alloy semiconductor $Cd_xZn_{1-x}Se$ during the fusion process, with the value of x determined by the ZnSe : CdSe ratio in the original melt. The band gap of the alloy can be 'tuned' through the visible spectrum region by varying x, and this determines the short wavelength transmission cut-off for the filter.

(2) The size of the semiconductor crystallites within the glass can be very small, and this can also have an effect on the colour produced. Normally, the optical properties of a material are independent of the size of the crystal, but this ceases to be the case if the dimensions are comparable to the electron wavelength. The 'quantum size effect' increases the energy of the electrons and hence shifts the effective band gap to higher energy. This point will be explained further in Section 6.9 of Chapter 6.

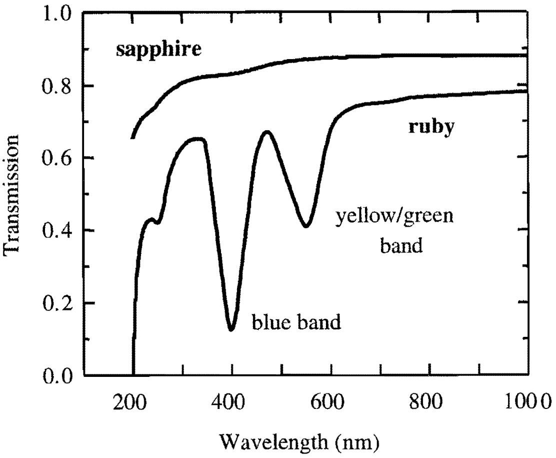

Fig. 1.7 Transmission spectrum of ruby (Al_2O_3 with 0.05 % Cr^{3+}) compared to sapphire (pure Al_2O_3). The thicknesses of the two crystals were 6.1 mm and 3.0 mm respectively. After [6], reprinted with permission.

The principle of doping optically active atoms into colourless hosts is employed extensively in the crystals used for solid state lasers. A typical example is the ruby crystal. Rubies consist of Cr^{3+} ions doped into Al_2O_3 (sapphire). In the natural crystals, the Cr^{3+} ions are present as impurities, but in synthetic crystals, the dopants are deliberately introduced in controlled quantities during the crystal growth process.

Figure 1.7 compares the transmission spectra of synthetic ruby (Al_2O_3 with 0.05 % Cr^{3+}) to that of synthetic sapphire (pure Al_2O_3). It is seen that the presence of the chromium ions produces two strong absorption bands, one in the blue spectral region and the other in the green/yellow region. These two absorption bands give rubies their characteristic red colour. The other obvious difference between the two transmission curves is that the overall transmission of the ruby is lower. This is caused in part by the increased scattering of light by the impurities in the crystal.

The optical properties of crystals like ruby will be covered in Chapter 9. We will see there that the broadening of the discrete transition lines of the isolated dopant ions into absorption bands is caused by vibronic coupling between the valence electrons of the dopant and the phonons in the host crystal. We will also see how the centre wavelength of the bands is determined by the crystal field effect, that is, the interaction between the dopant ions and electric field of the host crystal. These properties are very important in the design of solid state lasers and phosphors.

1.5 Characteristic optical physics in the solid state

The previous section has given a brief overview of the optical properties of several different classes of solid state materials. It is natural to ask whether any of these properties are exclusive to the solid state. In other words, how do the optical properties of a solid differ from those of its constituent atoms or molecules? This question is essentially the same as asking what the difference is between solid state and atomic or molecular physics.

The answer clearly depends on the type of material that we are considering. In some materials there will be a whole range of new effects associated with the solid state, while with others, the differences may not be so great. Molecular materials are an example of the second type. We would expect the absorption spectra of a solid film and that of an equivalent dilute solution to be very similar. This happens because the forces between the molecules in the condensed phase are relatively weak compared to the forces within the molecule itself. The appeal of the solid state in this case is the high number density of molecules that are present, and the possibility of incorporating them into solid state electronic devices.

With many other materials, however, there will be substantial differences between the condensed phase and the gaseous or liquid state. It is obviously not possible to give a full catalogue of these effects in an introductory chapter such as this one. Instead, we will highlight here five aspects that make the physics of the solid state interesting and different, namely

- Crystal symmetry
- Electronic bands
- Vibronic bands
- The density of states
- Delocalized states and collective excitations.

There are many others, of course, but these themes occur over and over again and are therefore worth considering briefly in themselves before we start going into the details.

1.5.1 Crystal symmetry

Most of the materials that we will be studying occur as crystals. Crystals have long range **translational order**, and can be categorized into 32 classes according to their **point group symmetry**. The point group symmetry refers to the group of symmetry operations that leaves the crystal invariant. Examples of these include rotations about particular axes, reflections about planes, and inversion about points in the unit cell. Some crystal classes such as the cubic ones possess a very high degree of symmetry. Others have much lower symmetry.

The link between the measurable properties and the point group symmetry of a crystal can be made through **Neumann's principle**. This states that:

> *Any macroscopic physical property must have at least the symmetry of the crystal structure.*

For example, if a crystal has four-fold rotational symmetry about a particular axis, then we must get the same result in any experiment we might perform in the four equivalent orientations.

It is instructive to compare the properties of a crystal to those of the atoms from which it has been formed. A gas of atoms has no translational order. Therefore we expect to find new effects in the solid state that reflect its translational symmetry. The formation of electronic bands and delocalized states discussed in Sections 1.5.2 and 1.5.5 below are examples of this. At the same time, the point group symmetry of a crystal is lower than that of the individual

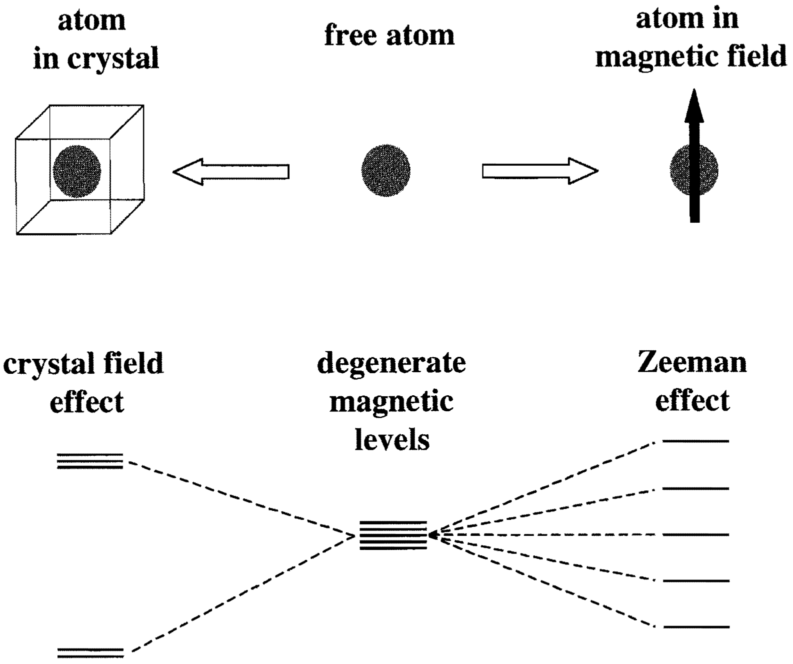

Fig. 1.8 Splitting of the magnetic levels of a free atom by the crystal field effect. In the free atoms, the magnetic levels are degenerate. We must apply a magnetic field to split them by the Zeeman effect. However, the magnetic levels can be split even without applying an external magnetic field in a crystal. The details of the way the levels split are determined by the symmetry class of the crystal.

atoms, which have the highest possible symmetry due to their spherical invariance. We therefore expect to find other effects in the solid state that relate to the lowering of the symmetry on going from free atoms to the particular point group of the crystal class. Two specific examples of this are discussed briefly here, namely **optical anisotropy** and the **lifting of degeneracies**.

A crystal is said to be anisotropic if its properties are not the same in all directions. Anisotropy is only found in the solid state, because gases and liquids do not have any preferred directions. The degree of anisotropy found in a crystal depends strongly on the point group symmetry that it possesses. In cubic crystals, for example, the optical properties must be the same along the x, y and z axes because they are physically indistinguishable. On the other hand, in a uniaxial crystal, the properties along the optic axis will be different from those along the axes at right angles to it. The optical anisotropy is manifested by the property of birefringence which is discussed in Section 2.4. It is also important for the description of the nonlinear optical coefficients of crystals discussed in Chapter 11.

The lifting of degeneracies by reduction of the symmetry is a well-known effect in atomic physics. Free atoms are spherically symmetric and have no preferred directions. The symmetry can be broken by applying an external magnetic or electric field which creates a preferred axis along the field direction. This can lead to the lifting of certain level degeneracies that are present in the free atoms. The Zeeman effect, for example, describes the splitting of degenerate magnetic levels when a magnetic field is applied. If the same atom is introduced into a crystal, it will find itself in an environment with a point group symmetry determined by the lattice. This symmetry is lower than that of the free atom, and therefore some level degeneracies can be lifted.

This point is illustrated schematically in Fig. 1.8, which shows how the magnetic levels of a free atom can be split by the crystal field effect in an analogous way to the Zeeman effect. The splitting is caused by the interaction of the orbitals of the atoms with the electric fields of the crystalline environment. The details do not concern us here. The important point is that the splittings are determined by the symmetry class of the crystal and do not require an external field. Optical transitions between these crystal-field split levels often occur in the visible spectral region, and cause the material to have very interesting properties that are not found in the free atoms. These effects will be explored in more detail in Chapter 9.

Before closing this section on crystal symmetry, it is worth pointing out that many important solid state materials do not possess long range translational symmetry. Glass is an obvious example. Other examples include thin molecular films such as light-emitting polymers sputtered onto substrates, and amorphous silicon. The optical properties of these materials may be very similar to those of their constituent atoms or molecules. Their importance is usually related to the convenience of the solid phase rather than to new optical properties that relate to the solid state physics.

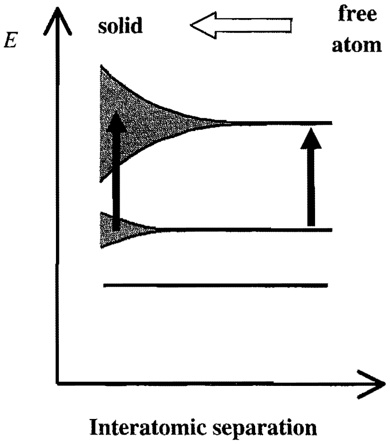

Fig. 1.9 Schematic diagram of the formation of electronic bands in a solid from the condensation of free atoms. As the atoms are brought closer together to form the solid, their outer orbitals begin to overlap with each other. These overlapping orbitals interact strongly, and broad bands are formed. The inner core orbitals do not overlap and so remain discrete even in the solid state. Optical transitions between the bands can occur, and this causes strong absorption over a continuous range of frequencies rather than discrete lines.

1.5.2 Electronic bands

The atoms in a solid are packed very close to each other, with the interatomic separation approximately equal to the size of the atoms. Hence the outer orbitals of the atoms overlap and interact strongly with each other. This broadens the discrete levels of the free atoms into bands, as illustrated schematically in Fig. 1.9.

The electron states within the bands are delocalized and possess the translational invariance of the crystal. Bloch's theorem states that the wave functions should be written in the form:

$$\psi_{\mathbf{k}}(\mathbf{r}) = u_{\mathbf{k}}(\mathbf{r}) \exp(i\mathbf{k} \cdot \mathbf{r}) \, , \tag{1.27}$$

where $u_{\mathbf{k}}(\mathbf{r})$ is a function that has the periodicity of the lattice. The Bloch states described by eqn 1.27 are modulated plane waves. Each electronic band has a different envelope function $u_{\mathbf{k}}(\mathbf{r})$ which retains some of the atomic character of the states from which the band was derived.

Optical transitions can occur between the electronic bands if they are allowed by the selection rules. This 'interband' absorption is possible over a continuous range of photon energies determined by the lower and upper energy limits of the bands. This contrasts with the absorption spectra of free atoms, which consist of discrete lines. The observation of broad bands of absorption rather than discrete lines is one of the characteristic features of the solid state.

Interband transitions will be discussed at length in a number of chapters in this book, most notably Chapters 3 and 5. The absorption strength is usually very high because of the very large density of absorbing atoms in the solid. This means that we can produce sizeable optical effects in very thin samples, allowing us to make the compact optical devices that form the basis of the modern optoelectronics industry.

1.5.3 Vibronic bands

The electronic states of the atoms or molecules in a solid may be strongly coupled to the vibrational modes of the crystal through the vibronic interaction. A typical example of where this effect occurs is the doped insulator crystals introduced in Section 1.4.5. The vibronic coupling broadens the discrete electronic states of the isolated dopant atoms into bands. This has the effect of broadening the discrete absorption and emission lines of the atoms into continuous bands. These vibronic effects will be described in more detail in Chapter 9.

It is important to realize that the reason for the formation of the vibronic bands is different to that for the electronic bands considered in the previous section. In the case of vibronic bands, the continuum of states arises from the coupling of discrete electronic states to a continuous spectrum of vibrational modes. This contrasts with the electronic bands, where the continuum arises from interactions between electronic states of neighbouring atoms.

Vibronic effects are also observed in molecular materials. This is an interesting case which highlights the difference between the solid state and the liquid or gaseous phase. The absorption spectra of simple free molecules also show vibrational–electronic bands, but the transition frequencies are discrete because both the electronic energies and the vibrational energies are discrete. In molecular solids, by contrast, the vibrational frequencies are continuous, and this causes continuous absorption and emission spectra.

1.5.4 The density of states

The concept of the **density of states** is an inevitable corollary of band formation in solids. The electronic and vibrational states of free molecules and atoms have discrete energies, but this is not the case in a solid: both the electronic states and the phonon modes have a continuous range of energies. This continuum of states leads to continuous absorption and emission bands, as has already been stressed in the previous two sections.

The number of states within a given energy range of a band is conveniently expressed in terms of the density of states function $g(E)$. This is defined as:

$$\text{Number of states in the range } E \rightarrow (E + dE) = g(E)\,dE\ . \tag{1.28}$$

$g(E)$ is worked out in practice by first calculating the density of states in momentum space $g(k)$, and then using the relationship between $g(E)$ and $g(k)$, namely:

$$g(E) = g(k)\frac{dk}{dE}\ . \tag{1.29}$$

This can be evaluated from knowledge of the E-k relationship for the electrons or phonons. Knowledge of $g(E)$ is crucial for calculating the absorption and emission spectra due to interband transitions and also for calculating the shape of vibronic bands.

1.5.5 Delocalized states and collective excitations

The fact that the atoms in a solid are very close together means that it is possible for the electron states to spread over many atoms. The wave functions of these delocalized states possess the underlying translational symmetry of the crystal. The Bloch waves described by eqn 1.27 are a typical example. The delocalized electron waves move freely throughout the whole crystal and interact with each other in a way that is not possible in atoms. The delocalization also allows collective excitations of the whole crystal rather than individual atoms. Two examples that we will consider in this book are the excitons formed from delocalized electrons and holes in a semiconductor, and the plasmons formed from free electrons in metals and doped semiconductors. These collective excitations may be observed in optical spectra, and have no obvious counterpart in the spectra of free atoms. These excitonic effects will be discussed in Chapter 4, while plasmons are covered in Section 7.5.

Other wave-like excitations of the crystal are delocalized in the same way as the electrons. In the case of the lattice vibrations, the delocalized excitations are described by the phonon modes. We have already mentioned above that the phonon frequencies are continuous, which contrasts with the discrete vibrational frequencies of molecules. Some optical effects related to phonons have direct analogies with the vibrational phenomena observed in isolated molecules but others are peculiar to the solid state. Examples of the former are Raman scattering and infrared absorption. Examples of the latter include the phonon-assisted interband transitions in semiconductors with indirect band gaps (cf. Section 3.4), and the broadening of the discrete levels of impurity atoms into continuous vibronic bands by interactions with phonons as discussed in Chapter 9.

The delocalized states of a crystal are described by quantum numbers such as $\mathbf{k}$ and $\mathbf{q}$ which have the dimensions of inverse length. These quantum numbers follow from the translational invariance, and are therefore a fundamental manifestation of the crystal symmetry. To all intents and purposes, the quantum numbers like $\mathbf{k}$ and $\mathbf{q}$ behave like the wave vectors of the excitations, and they will be treated as such whenever we encounter them in derivations. However, it should be borne in mind that this is really a consequence of the deep underlying symmetry which is unique to the solid state.

1.6 Microscopic models

In the following chapters we will be developing many microscopic models to explain the optical phenomena that are observed in the solid state. The types of models will obviously vary considerably, but they can all be classified into one of the following three general categories:

- Classical
- Semiclassical
- Fully quantum.

These approaches get progressively more difficult, and so we usually apply them in the order listed above.

In the classical approach we treat both the medium and the light according to classical physics. The dipole oscillator model described in Chapter 2 is a typical example. This model is the basic starting point for understanding the general optical properties of a medium, and in particular for describing the main effects due to free electrons (Chapter 7) and phonons (Chapter 10). We will also use it as a starting point for the discussion of nonlinear optics in Chapter 11. It would be a mistake to undervalue the classical approach in this modern day and age. The value of more sophisticated models will only be appreciated fully once the classical physics has been properly understood.

In semiclassical models we apply quantum mechanics to the atoms, but treat the light as a classical electromagnetic wave. The treatment of interband absorption in Chapter 3 is a typical example. The absorption coefficient is calculated using Fermi's golden rule, which requires knowledge of the wave functions of the quantized levels of the atoms, but treats the light–matter interaction as that between a quantized atom and a classical electric field wave. This semiclassical approach is used extensively throughout the book. Appendix B summarizes the main results that will be needed.

The final approach is the full quantum treatment. This is the realm of **quantum optics**, where both the atoms and the light are treated quantum mechanically. We use this approach implicitly whenever we refer to the light as a beam of photons and draw Feynman diagrams to represent the interaction processes that are occurring. This might give the impression that the explanations we are giving are fully quantum because we speak in terms of photons interacting with atoms. However, in the equations used to describe the process quantitatively, the light is treated classically and only the atoms are quantized. The quantitative description is therefore only semiclassical. The use of the fully quantum approach at the quantitative level is beyond the scope of this present book.

Chapter summary

- The propagation of light though a medium is quantified by the complex refractive index $\tilde{n}$. The real part of $\tilde{n}$ determines the velocity of light in the medium, while the imaginary part determines the absorption coefficient. Beer's law (eqn 1.4) shows that the intensity of light in an absorbing medium decays exponentially.
- Reflection occurs at the interface between two optical materials with different refractive indices. The coefficient of reflectivity can be calculated from the complex refractive index using eqn 1.26.
- The transmission of a sample is determined by the reflectivities of the surfaces and the absorption coefficient through eqn 1.6.
- The complex refractive index is related to the complex dielectric constant through eqn 1.19. The relationships between the real and imaginary parts of $\tilde{n}$ and $\tilde{\epsilon}_r$ are given in eqns 1.20–1.25.
- Luminescent materials re-emit light by spontaneous emission after absorbing photons. The frequency shift between the emission and absorption is called the Stokes shift.
- Scattering causes beam attenuation in accordance with Beer's law. The scattering is called elastic if the frequency is unchanged, and inelastic otherwise.

- The optical spectra of solid state materials usually consist of broad bands rather than sharp lines. The bands arise either from electronic interactions between neighbouring atoms or from vibronic coupling to the phonon modes.
- Insulators and glasses have vibrational absorption at infrared wavelengths and electronic absorption in the ultraviolet spectral region. They are transparent and colourless in the visible spectral region between these two absorption bands. In semiconductors and molecular materials the electronic absorption occurs at lower frequencies in the near infrared or visible spectral region.
- The free carriers present in metals make them highly reflective in the infrared and visible spectral regions. The colouration of some metals is caused by electronic interband absorption.
- The addition of optically active dopants to a colourless host crystal or glass produces the characteristic colours of stained glasses and gemstones.
- Crystals have both translational symmetry and point group symmetry. The consequences of the point group symmetry for the optical properties are determined by Neumann's principle.

Further reading

A good general discussion of the optical properties of materials can be found in Hecht (1998). A more advanced treatment may be found in Born and Wolf (1999). The introduction to the optical properties of various materials given in Section 1.4 will be expanded in subsequent chapters, where suitable further reading will be suggested.

The relationship between the optical properties and the complex refractive index and dielectric constant is discussed in most texts on electromagnetism, for example, Bleaney and Bleaney (1976), or Lorrain, Corson and Lorrain (2000). This material is also covered in Born and Wolf (1999).

A classic discussion of the effects of the point group symmetry on the physical properties of crystals is given in Nye (1957).

References

[1] Driscoll, W.G. and Vaughan, W. (1978). *Handbook of optics.* McGraw-Hill, New York.

[2] Kaye, G.W.C and Laby, T.H. (1986). *Tables of physical and chemical constants* (15th edn). Longman Scientific, Harlow, Essex.

[3] Madelung, O. (1996). *Semiconductors, basic data* (2nd edn). Springer-Verlag, Berlin.

[4] Lide, D.R. (1996). *CRC handbook of chemistry and physics* (77th edn). CRC Press, Boca Raton.

[5] Buckley, A.R., Rahn, M.D., Hill, J., Cabanillas-Gonzales, J., Fox, A.M. and Bradley, D.D.C. (2001). *Chem. Phys. Lett.*, **339**, 331.

[6] McCarthy, D.E. (1967). *Applied Optics*, **6**, 1896.

Exercises

(1.1) Crown glass has a refractive index of 1.51 in the visible spectral region. Calculate the reflectivity of the air–glass interface, and the transmission of a typical glass window.

(1.2) Use the data in Table 1.4 to calculate the ratio of the reflectivities of fused silica and dense flint glass.

(1.3) The complex dielectric constant of the semiconductor cadmium telluride is given by $\tilde{\epsilon}_r = 8.92 + i\,2.29$ at 500 nm. Calculate for CdTe at this wavelength: the phase velocity of light, the absorption coefficient and the reflectivity.

(1.4) The detectors used in optical fibre networks operating at 850 nm are usually made from silicon, which has an absorption coefficient of $1.3 \times 10^5\,\mathrm{m}^{-1}$ at this wavelength. The detectors have coatings on the front surface that makes the reflectivity at the design wavelength negligibly small. Calculate the thickness of the active region of a photodiode designed to absorb 90 % of the light.

(1.5) GaAs has a refractive index of 3.68 and an absorption coefficient of $1.3 \times 10^6\,\mathrm{m}^{-1}$ at 800 nm. Calculate the transmission coefficient and optical density of a $2\,\mu$m thick GaAs sample.

(1.6) Sea water has a refractive index of 1.33 and absorbs 99.8 % of red light of wavelength 700 nm in a depth of 10 m. What is its complex dielectric constant at this wavelength?

(1.7) How would you expect the absorption coefficient of a yellow colour glass filter to vary with wavelength?

(1.8) A beam of light is incident on a parallel-sided plate of thickness l as shown in Fig. 1.10. The reflectivity of the front and back surfaces is R and the absorption coefficient is α.

(i) Show that the intensity of the beam exiting the sample after having been reflected from the back surface once is smaller than that of the beam that has suffered no reflections by a factor $R^2\mathrm{e}^{-2\alpha l}$.

(ii) Calculate this ratio for a transparent glass window with a refractive index of 1.5.

(iii) Repeat part (ii), but calculate the ratio of the electric fields of the beams rather than their intensities.

(iv) Explain why the ratio of the fields might be important rather than the ratio of the intensities.

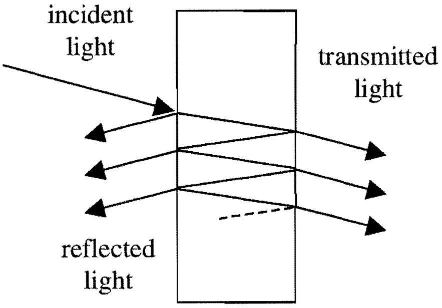

Fig. 1.10 Multiple reflections in a parallel-sided plate.

(1.9) Repeat Exercise 1.8(ii) and (iii) for the GaAs plate considered in Exercise 1.5.

(1.10) Show that the optical density (O.D.) of a sample is related to its transmission T and reflectivity R through:

$$\mathrm{O.D.} = -\log_{10}(T) + 2\log_{10}(1-R)\,.$$

Hence explain how you would determine the optical density by making two transmission measurements, one at wavelength λ where the material absorbs, and the other at a wavelength λ' where the material is transparent.

(1.11) The refractive index of fused silica is 1.45248 at 850 nm and 1.44427 at 1500 nm. Calculate the difference in time taken for short light pulses at 850 nm and 1500 nm to propagate down a silica optical fibre of length 1 km.

(1.12) The complex dielectric constant of a metal at infrared frequencies is given by

$$\tilde{\epsilon}_r = \epsilon_r + i\frac{\sigma}{\epsilon_0\omega}\,,$$

where ϵ_r is the static relative dielectric constant, σ is the electrical conductivity, and ω is the angular frequency. (See eqn A.45 in Appendix A with $\mu_r = 1$.) Estimate the reflectivity of a silver mirror at a wavelength of $100\,\mu$m. Assume that $\epsilon_2 \gg \epsilon_1$, and that the conductivity of silver is $6.6 \times 10^7\,\Omega^{-1}\mathrm{m}$.

(1.13) Estimate the distance over which the light intensity falls by a factor of 2 in a gold film at a wavelength of 100 μm. The electrical conductivity of gold is $4.9 \times 10^7 \, \Omega^{-1}$m. Make the same assumptions as in the previous question.

(1.14) The data shown in Fig. 1.5 indicates that the reflectivity of silver is close to zero at around 320 nm. What is the approximate value of the complex dielectric constant at this wavelength?

(1.15) A neodymium laser crystal absorbs photons at 850 nm and luminesces at 1064 nm. The efficiency of the luminescence process is quantified in terms of the radiative quantum efficiency η_R, which is defined as the fraction of the atoms that emit a photon after absorbing a photon.

(i) Calculate the amount of energy dissipated as heat in each emission process.

(ii) If the total power absorbed at 850 nm is 10 W, calculate the power emitted at 1064 nm if $\eta_R = 100$ %. How much power is dissipated as heat in the crystal?

(iii) Repeat part (ii) for a crystal with $\eta_R = 50$ %.

(1.16) A photon of wavelength 514 nm is scattered inelastically from an NaCl crystal by exciting a phonon of frequency 7.92×10^{12} Hz. By applying the law of conservation of energy to the scattering process, calculate the wavelength of the scattered photon.

(1.17) A certain optical fibre transmits 10 % of the light coupled into it at 850 nm. Calculate the transmission of the same fibre at 1550 nm, on the assumption that the dominant loss is Rayleigh scattering from inhomogeneities in the fibre. Hence explain why telecommunications companies use a wavelength of 1550 nm for their long distance optical fibre networks instead of the wavelength of 850 nm used for local area networks.

(1.18) Calculate the distance over which the intensity falls to 50 % of its original value in a medium which contains $10^{16}\,\text{m}^{-3}$ scattering centres with $\sigma_s = 2 \times 10^{-17}\,\text{m}^2$. Calculate the equivalent distance at half the wavelength, on the assumption that the Rayleigh scattering law applies.

(1.19) Explain why ice is birefringent, but water is not.

Classical propagation

2

The propagation of light through an optical medium was discussed in general terms in Sections 1.1–1.3 of Chapter 1. We saw there that the propagation is characterized by two parameters, namely the refractive index and the absorption coefficient. In this chapter we will investigate the classical theory of optical propagation, in which the light is treated as electromagnetic waves and the atoms or molecules are modelled as classical dipole oscillators. We will see that this model gives a good general overview of the optical properties, and enables us to calculate the frequency dependence of the complex dielectric constant. This gives us the frequency dependence of the absorption coefficient and refractive index, and hence enables us to explain the phenomenon of dispersion. We will also see that the model provides the framework for describing the effects due to optical anisotropy such as birefringence.

The treatment given here presupposes a working knowledge of the electromagnetic properties of dielectrics. A summary of the main results that we will use is given in Appendix A. The model will be revisited in subsequent chapters when we consider the optical properties of free electrons in Chapter 7, and when we discuss lattice vibrations in Chapter 10. The model is also the starting point for the treatment of nonlinear optical effects in Chapter 11.

2.1 Propagation of light in a dense optical medium

The classical model of light propagation was developed at the end of the nineteenth century following Maxwell's theory of electromagnetic waves and the introduction of the concept of the dipole oscillator. In this section we will give a qualitative discussion of the physical assumptions of this model, leaving the quantitative calculation to the next section.

The model assumes that there are several different types of oscillators within a medium, each with their own characteristic resonant frequency. At optical frequencies the most important contribution is from the oscillations of the **bound electrons** within the atoms, and so we begin this section by considering atomic oscillators. We then go on to introduce the idea of **vibrational oscillators**, which resonate at lower frequencies in the infrared spectral region, and finally mention **free electron oscillators**, which are responsible for the principal optical properties of metals.

2.1.1 Atomic oscillators

The concept of the dipole oscillator was introduced soon after Maxwell's electromagnetic theory. It was shown theoretically that an oscillating electric dipole would emit electromagnetic waves, and this was confirmed in 1887 when Heinrich Hertz succeeded in generating and detecting radio waves in the laboratory. He used an oscillatory discharge across a spark gap as the source and a wire loop as the aerial of the detector. This was an elegant confirmation of the validity of Maxwell's electromagnetic theory, and the beginning of radio telecommunications.

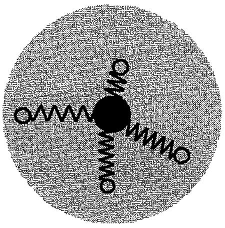

Fig. 2.1 Classical model of the bound electrons in an atom. The electrons are represented by the open circles, while the black circle at the centre of the atom represents the nucleus. The electrons are held to the heavy nucleus by springs which represent the restoring forces due to the binding between them. Each atom has a series of characteristic resonant frequencies which we now know to correspond with the quantized transition energies.

The idea of considering atoms as oscillating dipoles was originally proposed by Henrick Antoon Lorentz in 1878, thus preceding Hertz's demonstration by several years. It was known that atoms emit and absorb at discrete frequencies, and Lorentz's model provided a simple explanation for these observations in terms of the newly discovered electromagnetic theories.

The oscillator model of the atom is illustrated schematically in Fig. 2.1. It is assumed that the electron is held in a stable orbit with respect to the nucleus, and the spring represents the restoring force for small displacements from the equilibrium. The negatively charged electron and the positively charged nucleus form an electric dipole with a magnitude proportional to their separation. Lorentz, of course, could not have known about electrons and nuclei, because they were not discovered until 1897 and 1911 by J.J. Thomson and Ernest Rutherford respectively. Lorentz simply postulated the existence of dipoles without knowing their origin.

The natural resonant frequency ω_0 of the atomic dipoles is determined by their mass and the magnitude of the restoring force experienced for small displacements. The appropriate mass is the **reduced mass** given by:

$$\frac{1}{\mu} = \frac{1}{m_0} + \frac{1}{m_{\mathrm{N}}}, \tag{2.1}$$

where m_0 and m_{N} are the masses of the electron and nucleus respectively. Since $m_{\mathrm{N}} \gg m_0$, we may safely take $\mu \approx m_0$ here. The restoring force is quantified in terms of a spring constant K_{s}, which is chosen so that ω_0 coincides with one of the natural frequencies of the atoms (see Exercise 2.1):

$$\omega_0 = \sqrt{\frac{K_{\mathrm{s}}}{\mu}}. \tag{2.2}$$

We have to suppose that there are several dipoles within every atom, to account for the fact that a given atom has many transition frequencies. These are known from the absorption and emission spectra, and the frequencies occur in the near-infrared, visible and ultraviolet spectral regions (10^{14}–10^{15} Hz).

We can understand the connection between the atomic dipoles and the emission spectra by considering the oscillations of the dipole shown in Fig. 2.2. An electric dipole consists of a positive charge $+q$ at position $\mathbf{r}_+$ and a negative charge $-q$ at $\mathbf{r}_-$. The electric dipole moment is defined as

$$\mathbf{p} = q(\mathbf{r}_+ - \mathbf{r}_-). \tag{2.3}$$

Hence the positive nucleus and negative electron form a dipole with magnitude equal to $e|\mathbf{r}_{\mathrm{N}} - \mathbf{r}_{\mathrm{e}}|$.

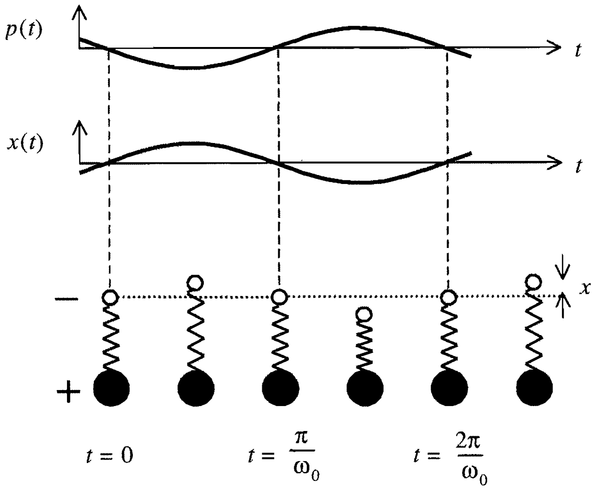

Fig. 2.2 Oscillations of a classical dipole consisting of a heavy positive charge and a light negative charge bound together by a spring. $x(t)$ is the time-dependent displacement of the negative charge from its equilibrium position. The natural vibrations of the dipole about the equilibrium length at frequency ω_0 generate a time dependent dipole moment $p(t)$ as indicated in the top half of the figure.

During the oscillations of the atomic dipole, the nucleus remains more or less stationary due to its heavy mass, while the electron oscillates backwards and forwards at frequency ω_0. Hence the oscillations produce a time varying dipole in addition to any permanent dipole the atom may have. The magnitude of the time varying dipole is given by:

$$p(t) = -ex(t)\,, \tag{2.4}$$

where $x(t)$ is the time varying displacement of the electron from its equilibrium position. This connection between the electron displacement and the time dependent atomic dipole is illustrated in the top half of Fig. 2.2. The oscillating dipole radiates electromagnetic waves at frequency ω_0, in accordance with the theory of classical Hertzian dipoles. Hence the atom is expected to radiate light at its resonant frequency whenever sufficient energy is imparted to it to excite the oscillations.

We can also use the dipole model to understand how the atom interacts with an external electromagnetic wave at frequency ω. The AC electric field exerts forces on the electron and the nucleus and drives oscillations of the system at frequency ω. If ω coincides with one of the natural frequencies of the atom, then we have a resonance phenomenon. This induces very large amplitude oscillations, and transfers energy from the external wave to the atom. The atom can therefore absorb energy from the light wave if $\omega = \omega_0$. The absorption strength is characterized by the absorption coefficient α, and the intensity of the wave will decay exponentially according to Beer's law (eqn 1.4).

We assume here that the forces exerted by the electric fields are very small compared to the binding forces that hold the electrons to the nucleus. This approximation may not be valid if we are using a very powerful laser beam to excite the medium. If this is the case, then we are working in the regime of nonlinear optics. These effects are considered in Chapter 11.

We now know from quantum theory that what actually happens during absorption is that the atom jumps to an excited state by absorbing a photon. This can only occur if $\hbar\omega = E_2 - E_1$, where E_1 and E_2 are the quantized energies of the initial and final states. Once it has been excited, the atom can return to the ground state by a series of radiationless transitions, in which case the energy from the absorbed photon is ultimately converted into heat. Alternatively, it can luminesce by re-emitting a photon at some later time. The re-radiated photons are incoherent with each other and are emitted in all directions rather than in the specific direction of the incoming wave. Hence there is a net decrease in the energy flow in the beam direction, which is equivalent to absorption.

If ω does not coincide with any of the resonant frequencies, then the atoms will not absorb, and the medium will be transparent. In this situation the light wave drives non-resonant oscillations of the atoms at its own frequency ω. The oscillations of the atoms follow those of the driving wave, but with a phase lag. The phase lag is a standard feature of forced oscillators and is caused by damping. (See Exercise 2.2.) The oscillating atoms all re-radiate instantaneously, but the phase lag acquired in the process accumulates through the medium and retards the propagation of the wave front. This implies that the propagation velocity is smaller than in free space. The reduction of the velocity in the medium is characterized by the refractive index defined in eqn 1.2.

The slowing of the wave due to the non-resonant interactions can be considered as a repeated scattering process. The scattering is both coherent and elastic, and each atom behaves like a Huygens point source. The scattered light interferes constructively in the forward direction, and destructively in all other directions, so that the direction of the beam is unchanged by the repetitive scattering process. However, each scattering event introduces a phase lag which causes a slowing of the propagation of the phase front through the medium.

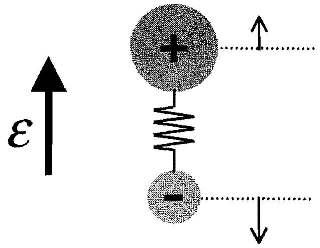

Fig. 2.3 Classical model of a polar molecule. The atoms are positively and negatively charged, and can vibrate about their equilibrium separation. These vibrations produce an oscillating electric dipole which will radiate electromagnetic waves at the resonant frequency. Alternatively, the molecule will interact with the electric field $\mathcal{E}$ of a light wave through the forces exerted on the charged atoms.

2.1.2 Vibrational oscillators

An optical medium may contain other types of dipole oscillators in addition to those originating from the bound electrons within the atoms. If the medium is ionic, it will contain oppositely charged ions. Vibrations of these charged atoms from their equilibrium positions within the crystal lattice will produce an oscillating dipole moment, in exactly the same way as the oscillations of the electrons within the individual atoms that we considered above. Therefore, we must also consider the optical effects dues to these vibrational oscillators when we consider the interaction of light with an ionic optical medium.

The optical effects of vibrational oscillators are well known in molecular physics. Figure 2.3 gives a schematic illustration of a classical polar molecule. This consists of two charged atoms bound together in a stable configuration, with the spring representing the molecular bond between them. The charged atoms can vibrate about their equilibrium positions and induce an oscillating electric dipole in an analogous way to the bound electrons in the atoms. We see immediately from eqn 2.2 that the vibrations will occur at lower frequencies because the reduced mass is larger. The vibrations therefore occur at infrared frequencies with $\omega/2\pi \sim 10^{12}$–10^{13} Hz. These molecular vibrations are associated with strong absorption lines in the infrared spectral region.

The interaction between the vibrations of the molecule and the light wave occurs through the forces exerted on the atoms by the electric field. It is obvious that this can only happen if the atoms are charged. This is why we specified that the molecule was polar in the preceding paragraph. A polar molecule is one in which the electron charge cloud that forms the bond sits closer to one of the atoms than to the other. Ionic molecules like the alkali halides (e.g. Na^+Cl^-) clearly fall into this category, while purely covalent ones such as the elemental molecules (e.g. O_2) do not. Many other molecules fall somewhere between these two limits. Water (H_2O) is a well known example. Oxygen has a greater electron affinity than hydrogen, and so the valence electrons in the O–H bond sit closer to the oxygen atoms. The two hydrogen atoms therefore possess a small positive charge which is balanced by a negative charge of twice the magnitude on the oxygen atom.

In a crystalline solid formed from the condensation of polar molecules, the atoms are arranged in an alternating sequence of positive and negative ions. The ions can vibrate about their equilibrium positions, and this produces oscillating dipole waves. These oscillations are associated with **lattice vibrations**, and they occur at frequencies in the infrared spectral region. We will consider the optical properties related to the lattice vibrations in detail in Chapter 10. We will see there that the light–matter interaction is associated with the excitation of **phonons**, which are quantized lattice waves. At this stage, we simply note that the lattice vibrations of a polar crystal give rise to strong optical effects in the infrared spectral region. These effects occur in addition to those due to the bound electrons of the atoms that comprise the crystal. In practice we can treat these two types of dipoles separately because the resonances are sharp and they occur at very different frequencies. Therefore the resonant effects of the bound electrons are negligible at the frequencies of the lattice vibrations, and *vice versa*. This point will be considered in more detail in Section 2.2.2.

2.1.3 Free electron oscillators

The electronic and vibrational dipoles considered above are both examples of bound oscillators. Metals and doped semiconductors, by contrast, contain significant numbers of **free electrons**. As the name implies, these are electrons that are not bound to any atoms, and therefore do not experience any restoring forces when they are displaced. This implies that the spring constant in eqn 2.2 is zero, and hence that the natural resonant frequency $\omega_0 = 0$.

The free electron model of metals is attributed to Paul Drude, and so the application of the dipole oscillator model to free electron systems is generally called the **Drude–Lorentz model**. The dipole oscillator model is perfectly valid, except that we must set $\omega_0 = 0$ throughout. The optical properties of free electron systems will be discussed in Chapter 7.

2.2 The dipole oscillator model

In the previous section we introduced the general assumptions of the dipole oscillator model. We now want to use the model to calculate the frequency dependence of the refractive index and absorption coefficient. This will provide a simple explanation for the dispersion of the refractive index in optical materials, and will also illustrate a very general point that the phenomena of absorption and refraction are related to each other.

2.2.1 The Lorentz oscillator

We consider the interaction between a light wave and an atom with a single resonant frequency ω_0 due to the bound electrons, as given by eqn 2.2. We model the displacement of the atomic dipoles as damped harmonic oscillators. The inclusion of damping is a consequence of the fact that the oscillating dipoles can lose their energy by collisional processes. In solids, this would typically occur through an interaction with a phonon which has been thermally excited in the crystal. As we will see, the damping term has the effect of reducing the peak absorption coefficient and broadening the absorption line.

We know from experimental observations that atoms must have many natural resonant frequencies to account for the multiplicity of lines in the absorption and emission spectra. However, the salient features of the physical behaviour are well illustrated by a singly resonant system, and the inclusion of multiple resonances complicates the discussion without adding much to the physical understanding at this stage. We therefore postpone the discussion of the effects of multiple resonances to subsection 2.2.2 below.

The electric field of the light wave induces forced oscillations of the atomic dipole through the driving forces exerted on the electrons. We make the assumption that $m_{\mathrm{N}} \gg m_0$ here so that we can ignore the motion of the nucleus. The displacement x of the electron is governed by an equation of motion of the form:

$$m_0 \frac{d^2x}{dt^2} + m_0\gamma \frac{dx}{dt} + m_0\omega_0^2 x = -e\mathcal{E}\,, \tag{2.5}$$

where γ is the damping rate, e is the magnitude of the electric charge of the electron, and $\mathcal{E}$ is the electric field of the light wave. The terms on the left hand side represent the acceleration, the damping and the restoring force respectively. The damping is modelled by a frictional force which is proportional to the velocity and impedes the motion. The term on the right hand side represents the driving force due to the AC electric field of the light wave.

We consider the interaction of the atom with a monochromatic light wave of angular frequency ω. The time dependence of the electric field is given by

$$\mathcal{E}(t) = \mathcal{E}_0 \cos(\omega t + \Phi) = \mathcal{E}_0 \Re\mathrm{e}\Big(\exp(-i\omega t - \Phi)\Big), \tag{2.6}$$

where $\mathcal{E}_0$ is the amplitude and Φ is the phase of the light. In order to keep consistency with the sign convention introduced later, we have chosen to take the negative frequency part of the complex exponential.

Note that the phase factors Φ and Φ' in eqns 2.6 and 2.7 are not necessarily the same. In fact, the phase of the electrons will tend to lag behind the phase of the light. This is a well known property of forced oscillations: the vibrations occur at the same frequency as the driving force but lag behind due to the damping term. This phase lag is the origin of the slowing down of the light in the optical medium, as discussed above in Section 2.1.

The AC electric field will drive oscillations at its own frequency ω. We therefore substitute eqn 2.6 into eqn 2.5 and look for solutions of the form:

$$x(t) = X_0 \Re\mathrm{e}\Big(\exp(-i\omega t - \Phi')\Big)\,, \tag{2.7}$$

where X_0 and Φ' are the amplitude and phase of the oscillations. We can incorporate the phase factors of eqns 2.6 and 2.7 into the amplitudes by allowing both $\mathcal{E}_0$ and X_0 to be complex numbers. We then substitute $\mathcal{E}(t) = \mathcal{E}_0\mathrm{e}^{-i\omega t}$ into eqn 2.5, and look for solutions of the form $x(t) = X_0\mathrm{e}^{-i\omega t}$. This gives:

$$-m_0\omega^2 X_0\mathrm{e}^{-i\omega t} - i m_0\gamma\omega X_0\mathrm{e}^{-i\omega t} + m_0\omega_0^2 X_0\mathrm{e}^{-i\omega t} = -e\mathcal{E}_0\mathrm{e}^{-i\omega t}\,, \tag{2.8}$$

which implies that:

$$X_0 = \frac{-e\mathcal{E}_0/m_0}{\omega_0^2 - \omega^2 - i\gamma\omega}\,. \tag{2.9}$$

The displacement of the electrons from their equilibrium position produces a time varying dipole moment $p(t)$, as shown in Fig. 2.2. The magnitude of the dipole is given by eqn 2.4. This gives a resonant contribution to the macroscopic polarization (dipole moment per unit volume) of the medium. If

N is the number of atoms per unit volume, the resonant polarization is given by:

$$\begin{aligned} P_{\text{resonant}} &= Np \\ &= -Nex \\ &= \frac{Ne^2}{m_0} \frac{1}{\left(\omega_0^2 - \omega^2 - i\gamma\omega\right)} \mathcal{E} . \end{aligned} \tag{2.10}$$

A quick inspection of eqn 2.10 shows that the magnitude of P_{resonant} is small unless the frequency is close to ω_0. This is another general property of forced oscillations: the response is small unless the frequency is close to resonance with the natural frequency of the oscillator.

Equation 2.10 can be used to obtain the complex relative dielectric constant ϵ_{r}. The electric displacement **D** of the medium is related to the electric field $\boldsymbol{\mathcal{E}}$ and polarization **P** through:

$$\mathbf{D} = \epsilon_0 \boldsymbol{\mathcal{E}} + \mathbf{P}, \tag{2.11}$$

where the bold font indicates vector quantities (see eqn A.2 in Appendix A). We are interested in the optical response at frequencies close to ω_0, and so we split the polarization into a non-resonant background term and the resonant term arising from the driven response of the oscillator. We therefore write:

$$\begin{aligned} \mathbf{D} &= \epsilon_0 \boldsymbol{\mathcal{E}} + \mathbf{P}_{\text{background}} + \mathbf{P}_{\text{resonant}} \\ &= \epsilon_0 \boldsymbol{\mathcal{E}} + \epsilon_0 \chi \boldsymbol{\mathcal{E}} + \mathbf{P}_{\text{resonant}} . \end{aligned} \tag{2.12}$$

The electric susceptibility χ in eqn 2.12 accounts for all other contributions to the polarizability of the atoms. We will discuss the physical meaning of the 'non-resonant polarization' in subsection 2.2.2 below.

To simplify the mathematics, we will assume that the material is isotropic, in which case the relative dielectric constant is defined through the relationship:

$$\mathbf{D} = \epsilon_0 \epsilon_{\text{r}} \boldsymbol{\mathcal{E}} . \tag{2.13}$$

We then combine eqns 2.10–2.13 to obtain:

$$\epsilon_{\text{r}}(\omega) = 1 + \chi + \frac{Ne^2}{\epsilon_0 m_0} \frac{1}{\left(\omega_0^2 - \omega^2 - i\gamma\omega\right)} . \tag{2.14}$$

The treatment of non-isotropic materials only introduces unnecessary complications at this stage, and will be covered briefly in Section 2.4.

This can be spilt into its real and imaginary parts according to eqn 1.18 to give:

$$\epsilon_1(\omega) = 1 + \chi + \frac{Ne^2}{\epsilon_0 m_0} \frac{\omega_0^2 - \omega^2}{(\omega_0^2 - \omega^2)^2 + (\gamma\omega)^2} \tag{2.15}$$

$$\epsilon_2(\omega) = \frac{Ne^2}{\epsilon_0 m_0} \frac{\gamma\omega}{(\omega_0^2 - \omega^2)^2 + (\gamma\omega)^2} . \tag{2.16}$$

These formulae can be simplified further if we are working at frequencies close to resonance, where $\omega \approx \omega_0 \gg \gamma$. This allows us to approximate $(\omega_0^2 - \omega^2)$ by $2\omega_0 \Delta\omega$, where $\Delta\omega = (\omega - \omega_0)$ is the detuning from ω_0. We then notice that the low and high frequency limits of $\epsilon_{\text{r}}(\omega)$ are given by

$$\epsilon_{\text{r}}(0) \equiv \epsilon_{\text{st}} = 1 + \chi + \frac{Ne^2}{\epsilon_0 m_0 \omega_0^2} , \tag{2.17}$$

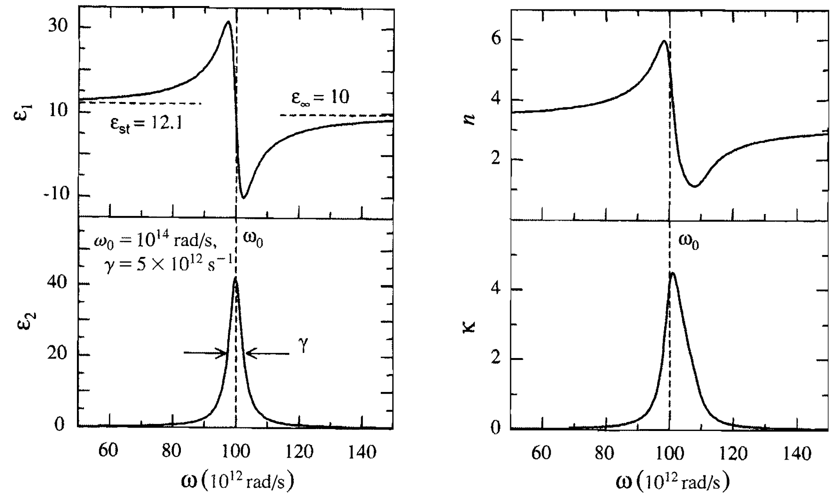

Fig. 2.4 Frequency dependence of the real and imaginary parts of the complex dielectric constant of a dipole oscillator at frequencies close to resonance. The graphs are calculated for an oscillator with $\omega_0 = 10^{14}$ rad/s, $\gamma = 5\times10^{12}\,\mathrm{s}^{-1}$, $\epsilon_{st} = 12.1$ and $\epsilon_\infty = 10$. Also shown is the real and imaginary part of the refractive index calculated from the dielectric constant.

and

$$\epsilon_r(\infty) \equiv \epsilon_\infty = 1 + \chi \tag{2.18}$$

respectively. The subscript on ϵ_{st} stands for 'static', since it represents the dielectric response to static electric fields. With this notation we find that:

$$(\epsilon_{st} - \epsilon_\infty) = \frac{Ne^2}{\epsilon_0 m_0 \omega_0^2}\,. \tag{2.19}$$

We finally rewrite eqns 2.15 and 2.16 in the following form valid at frequencies close to resonance:

$$\epsilon_1(\Delta\omega) = \epsilon_\infty - (\epsilon_{st} - \epsilon_\infty)\frac{2\omega_0\Delta\omega}{4(\Delta\omega)^2 + \gamma^2}\,, \tag{2.20}$$

$$\epsilon_2(\Delta\omega) = (\epsilon_{st} - \epsilon_\infty)\frac{\gamma\omega_0}{4(\Delta\omega)^2 + \gamma^2}\,. \tag{2.21}$$

These equations describe a sharp atomic absorption line centred at ω_0 with full width at half maximum equal to ν.

Figure 2.4 shows the frequency dependence of ϵ_1 and ϵ_2 predicted by eqns 2.20–2.21 for an oscillator with $\omega_0 = 10^{14}$rad/s, $\gamma = 5\times10^{12}\mathrm{s}^{-1}$, $\epsilon_{st} = 12.1$ and $\epsilon_\infty = 10$. These numbers are fairly typical of the infrared absorption lines in an ionic crystal. We see that ϵ_2 is a strongly peaked function of ω with a maximum value at ω_0 and a full width at half maximum equal to γ. The frequency dependence of ϵ_1 is more complicated. As we approach ω_0 from below, ϵ_1 gradually rises from the low frequency value of ϵ_{st}, and reaches a peak at $\omega_0 - \gamma/2$. (See Example 2.1.) It then falls sharply, passing through a minimum at $\omega_0 + \gamma/2$ before rising again to the high frequency limit of ϵ_∞. Note that the frequency scale over which these effects occur is determined by γ for both ϵ_1 and ϵ_2. This shows that the damping of the oscillator causes line broadening. The frequency dependence determined of ϵ_1 and ϵ_2 shown in Fig. 2.4 is called Lorentzian after the originator of the dipole model.

In an experiment we actually measure the refractive index n and the absorption coefficient α. The measurement of α then determines the extinction coefficient κ through eqn 1.16. Figure 2.4 shows the values of n and κ calculated from ϵ_1 and ϵ_2 using eqns 1.22 and 1.23. We see that n approximately follows the frequency dependence of $\sqrt{\epsilon_1(\omega)}$, while κ more or less follows $\epsilon_2(\omega)$. The correspondence $n \leftrightarrow \sqrt{\epsilon_1}$ and $\kappa \leftrightarrow \epsilon_2$ would be exact if κ were much smaller than n (cf. eqns 1.24 and 1.25). This is what generally happens in gases in which the low density of atoms makes the total absorption small. In the example shown in Fig. 2.4 the correspondence is only approximate because the absorption is very strong near ω_0, so that we cannot always assume $n \gg \kappa$. Nevertheless, the basic behaviour shows that the absorption peaks at a frequency very close to ω_0 and has a width of about γ, while the refractive index shows positive and negative excursions below and above ω_0. This is the typical behaviour expected of an atomic absorption line.

One interesting aspect of the Lorentz oscillator is that it affects the refractive index over a much larger frequency range than the absorption. This point is clearly shown in the graphs given in Fig. 2.4. The absorption is a strongly peaked function of ω and falls off as $(\Delta\omega)^{-2}$ as we tune away from resonance. Thus there is no significant absorption if we tune sufficiently far from resonance. On the other hand, the frequency dependence of the refractive index varies as $|\Delta\omega|^{-1}$ for large $|\Delta\omega|$. This follows from eqn 2.20 with the approximation $n = \sqrt{\epsilon_1}$, which is valid for large $|\Delta\omega|$ when ϵ_2 is very small.

Example 2.1

The full width at half maximum of the strongest hyperfine component of the sodium D_2 line at 589.0 nm is 100 MHz. A beam of light passes through a gas of sodium with an atom density of $1 \times 10^{17}\,\mathrm{m}^{-3}$. Calculate: (i) The peak absorption coefficient due to this absorption line. (ii) The frequency at which the resonant contribution to the refractive index is at a maximum. (iii) The peak value of the resonant contribution to the refractive index.

Solution

(i) We are dealing with a low density gas of atoms, and so the approximations given in eqns 1.24 and 1.25 will be valid. This means that the absorption will directly follow the frequency dependence of $\epsilon_2(\omega)$, and the peak absorption will occur precisely at the line centre. The peak extinction coefficient can be worked out from eqns 2.16 and 1.25. This gives:

$$\kappa(\omega_0) = \frac{\epsilon_2(\omega_0)}{2n} = \frac{Ne^2}{2n\epsilon_0 m_0}\frac{1}{\gamma\omega_0}.$$

We do not know what n is, but because we are dealing with a gas, it will only be very slightly different from unity. This point is confirmed in part (iii) of the question. We therefore take $n = 1$ here, and insert $N = 1 \times 10^{17}\,\mathrm{m}^{-3}$, $\gamma = 2\pi \times 10^8\,\mathrm{s}^{-1}$ and $\omega_0 = 2\pi c/\lambda = 3.20 \times 10^{15}$ rad/s to find that $\kappa(\omega_0) = 7.90 \times 10^{-5}$. This confirms that $n \gg \kappa$, and hence that it is valid to use eqn 1.25. We then work out the absorption coefficient from Eq. 1.16, which gives:

$$\alpha_{\max} \equiv \alpha(\omega_0) = \frac{4\pi\kappa(\omega_0)}{\lambda} = 1.7 \times 10^3\,\mathrm{m}^{-1}.$$

The absorption coefficient measured in an experiment would actually be smaller than the value calculated here by about a factor of 3. This discrepancy is caused by the fact that we are assuming that the oscillator strength of the transition is unity. This point is discussed further in section 2.2.2 below.

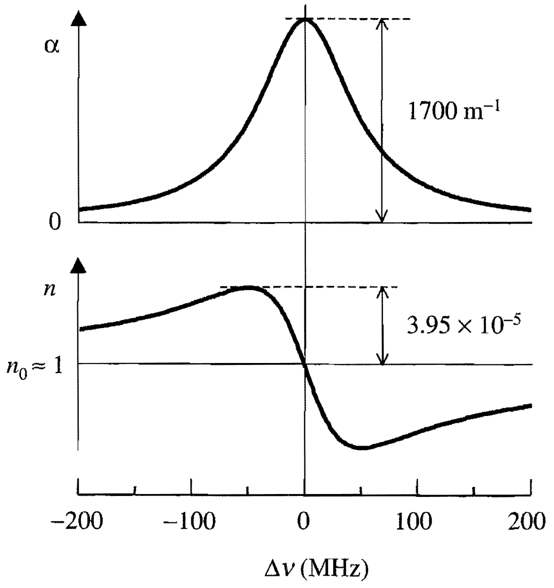

Fig. 2.5 Absorption coefficient and refractive index of sodium gas in the vicinity of the strongest hyperfine component of the D$_2$ line, on the assumption that the oscillator strength of the transition is unity, and that the atom density is 1×10^{17} m^{-3}. See Example 2.1 for the details. n_0 represents the off-resonant refractive index, which is approximately equal to unity.

(ii) We know from Fig. 2.4 that there will be a peak in the refractive index just below ω_0. Equation 1.24 tells us that $n(\omega) = \sqrt{\epsilon_1(\omega)}$, and hence that the local maximum of n will occur at the same frequency as the maximum in ϵ_1. Since the peak occurs near ω_0, it will be valid to use eqn 2.20. The local maximum occurs when:

$$\frac{d\epsilon_1(\omega)}{d\omega} \equiv \frac{d\epsilon_1(\Delta\omega)}{d\Delta\omega} \propto \frac{4(\Delta\omega)^2 - \gamma^2}{[4(\Delta\omega)^2 + \gamma^2]^2} = 0 .$$

This gives $\Delta\omega = \pm\gamma/2$. We see from Fig. 2.4 that $\Delta\omega = -\gamma/2$ corresponds to the local maximum, while $\Delta\omega = +\gamma/2$ corresponds to the local minimum. Therefore the peak in the refractive index occurs 50 MHz below the line centre.

(iii) From part (ii) we know that the local maximum in the refractive index occurs when $\Delta\omega = -\gamma/2$. We see from eqns 1.24 and 2.20 that the refractive index at this frequency is given by:

$$n_{\max} = \sqrt{\epsilon_1} = \left(\epsilon_\infty + \frac{Ne^2}{2\epsilon_0 m_0 \omega_0 \gamma}\right)^{\frac{1}{2}} = n_0\left(1 + \frac{7.90 \times 10^{-5}}{n_0^2}\right)^{\frac{1}{2}} ,$$

where $n_0 = \sqrt{\epsilon_\infty}$ is the off-resonant refractive index. We are dealing with a low density gas, and so it is justified to take $n_0 \approx 1$ here. This implies that the peak value of the resonant contribution to the refractive index is 3.95×10^{-5}.

The full frequency dependence of the absorption and refractive index near this absorption line is plotted in Fig. 2.5.

2.2.2 Multiple resonances

In general, an optical medium will have many characteristic resonant frequencies. We already discussed in Section 2.1 how we expect to observe separate resonances due to the lattice vibrations and to the oscillations of the bound electrons within the atoms. Furthermore, a particular medium may have many resonances of each type. We can treat these multiple resonances without difficulty in our model provided they occur at distinct frequencies.

In writing eqn 2.12 we split the polarization of the medium into a resonant part and a non-resonant part. We then discussed the resonant part in detail, without specifying very accurately what we meant by the non-resonant term. We simply stated that **P** was proportional to $\mathcal{E}$ through the susceptibility χ. In reality, the non-resonant polarization of the medium must originate from the polarizability of the atoms in exactly the same way as the resonant part. Equation 2.19 tells us that the dielectric constant decreases each time we go through an absorption line. The contributions that enter the background electric susceptibility χ in eqn 2.12 thus arise from the polarization due to all the other oscillators at higher frequencies.

We can understand this point better by making it more quantitative. The contribution to the polarization of a particular oscillator is given by eqn 2.10. In a medium with many electronic oscillators of different frequencies, the total polarization will therefore be given by

$$\mathbf{P} = \left(\frac{Ne^2}{m_0} \sum_j \frac{1}{\left(\omega_j^2 - \omega^2 - i\gamma_j\omega\right)} \right) \mathcal{E}, \qquad (2.22)$$

where ω_j and γ_j are the frequency and damping terms of a particular resonance line. We then substitute this into eqn 2.11, and recall the definition of ϵ_r given in eqn 2.13. This gives:

$$\epsilon_r(\omega) = 1 + \frac{Ne^2}{\epsilon_0 m_0} \sum_j \frac{1}{\left(\omega_j^2 - \omega^2 - i\gamma_j\omega\right)}. \qquad (2.23)$$

This equation takes account of all the transitions in the medium and can be used to calculate the full frequency dependence of the dielectric constant.

The refractive index and absorption coefficient calculated from eqn 2.23 are plotted against frequency in Fig. 2.6. The figure has been calculated for a hypothetical solid with three well-separated resonances with ω_j equal to 4×10^{13} rad/s, 4×10^{15} rad/s and 1×10^{17} rad/s respectively. The width of each absorption line has been set to 10 % of the centre frequency by appropriate choice of the damping term. The resonance in the infrared is included to represent the vibrational absorption. In a real solid, we would have to adapt the model appropriately to account for the different reduced mass and effective charge of the vibrational oscillator.

We can understand this figure by starting at the highest frequencies and gradually working our way down to the lower frequencies. At the very highest frequencies, the electrons are incapable of responding to the driving field. The medium therefore has no polarization, and the dielectric constant is unity. As we reduce the frequency, we first run into the transitions of the inner electrons in the X-ray/vacuum-ultraviolet spectral region, and then the transitions of the outer electrons in the ultraviolet and visible. We then have a region with no transitions until we finally reach the vibrational frequencies in the infrared. Each time we go through one of these resonances, we see the characteristic

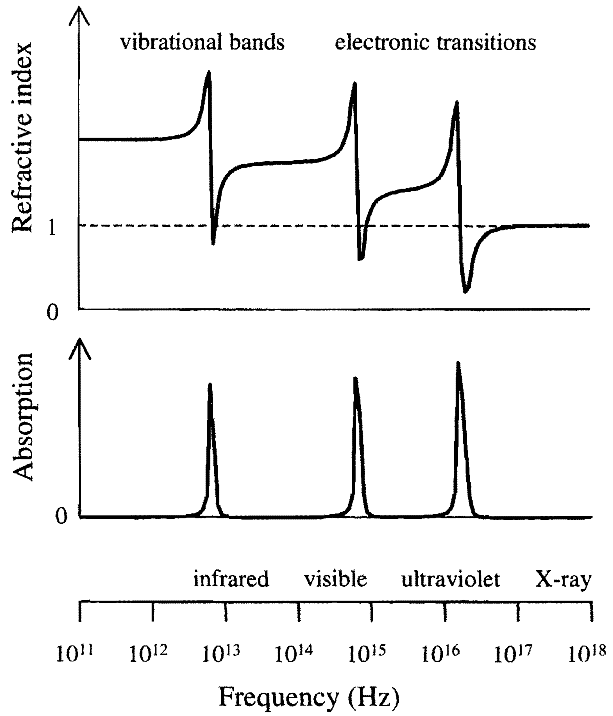

Fig. 2.6 Schematic diagram of the frequency dependence of the refractive index and absorption of a hypothetical solid from the infrared to the X-ray spectral region. The solid is assumed to have three resonant frequencies with $\omega_j = 4 \times 10^{13}$ rad/s, 4×10^{15} rad/s and 1×10^{17} rad/s respectively. The width of each absorption line has been set to 10 % of the centre frequency by appropriate choice of the γ_j's.

frequency dependence of the Lorentz oscillator, with a peak in the absorption spectrum and a 'wiggle' in the refractive index. In between the resonances the medium is transparent: the absorption coefficient is zero and the refractive index is almost constant.

The value of the refractive index in the transparent regions gradually increases as we go through more and more resonance lines on decreasing the frequency. This increase of the refractive index is caused by the fact that $\epsilon_{\text{st}} > \epsilon_\infty$ (cf. eqn 2.19), which implies that n is larger below an absorption line than above it. By reference to Fig. 2.6, we now see that we have to understand 'static' and '∞' as relative to a particular resonance. The variation of n with frequency due to the resonances is the origin of the dispersion found in optical materials even when they are transparent. This point will be discussed further in Section 2.3 below.

An astute reader will have noticed that the peak absorption coefficient for the three transition lines shown in Fig. 2.6 decreases slightly with decreasing frequency. This happens because n is larger at the lower frequencies. The transitions all have the same peak ϵ_2, but we can see from eqn 1.21 that κ must be slightly smaller if n is larger.

The dipole oscillator model predicts that each oscillator contributes a term given by eqn 2.10. This leads to a series of absorption lines of the same strength. However, experimental data shows that the absorption strength actually varies considerably between different atomic transitions. With the benefit of hindsight, we know that this is caused by the variation of the quantum mechanical transition probability. (See Appendix B.) In classical physics, however, there is no explanation, and we just assign a phenomenological **oscillator strength** f_j to each transition, rewriting eqn 2.23 as:

$$\epsilon_r(\omega) = 1 + \frac{Ne^2}{\epsilon_0 m_0} \sum_j \frac{f_j}{\left(\omega_{0j}^2 - \omega^2 - i\gamma_j\omega\right)}. \qquad (2.24)$$

It can be shown from quantum mechanics that we must have $\sum_j f_j = 1$ for each electron. Since the classical model predicts $f_j = 1$ for each oscillator, we then interpret this by saying that a particular electron is involved in several transitions at the same time, and the absorption strength is being divided between these transitions.

2.2.3 Comparison with experimental data

The schematic behaviour shown in Fig. 2.6 can be compared to experimental data on a typical solid state material. Figure 2.7 shows the frequency dependence of the refractive index and extinction coefficient of fused silica (SiO_2) glass from the infrared to the X-ray spectral region. The general characteristics indicated by Fig. 2.6 are clearly observed, with strong absorption in the infrared and ultraviolet, and a broad region of low absorption in between. The data confirms that $n \gg \kappa$ except near the peaks of the absorption. This means that the approximation whereby we associate the frequency dependence of n with that of ϵ_1, and that of κ with ϵ_2 (eqns 1.24 and 1.25), is valid at most frequencies.

The general behaviour shown in Fig. 2.7 is typical of optical materials which are transparent in the visible spectral region. We already noted in Sections 1.4.1 and 1.4.2 that the transmission range of colourless materials is determined by

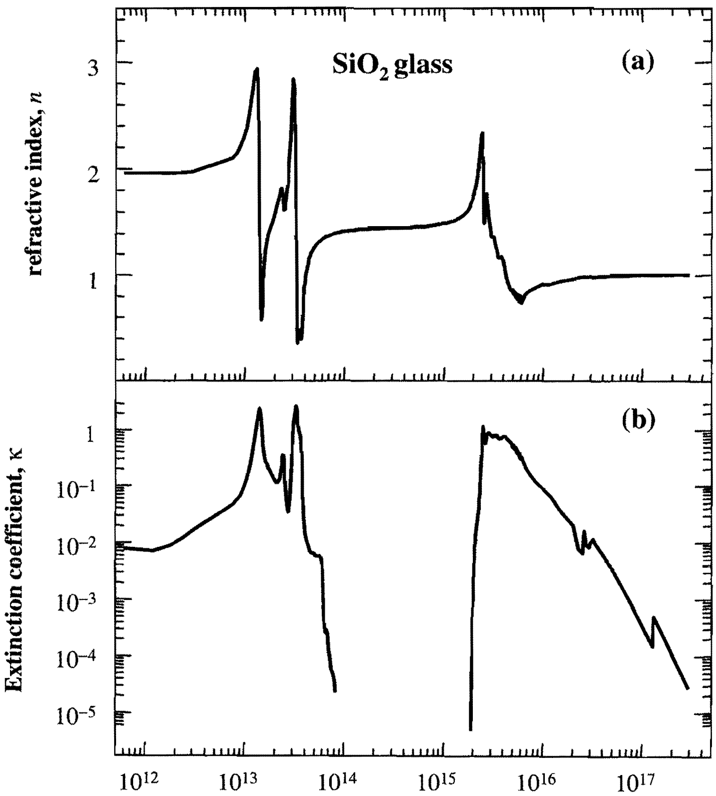

Fig. 2.7 (a) Refractive index and (b) extinction coefficient of fused silica (SiO_2) glass from the infrared to the x-ray spectral region. After [1].

the electronic absorption in the ultraviolet and the vibrational absorption in the infrared. This is demonstrated by the transmission data for sapphire shown in Fig. 1.4(a).

Silica is a glass, and hence does not have a regular crystal lattice. The infrared absorption is therefore caused by excitation of vibrational quanta in the SiO_2 molecules themselves. Two distinct peaks are observed at 1.4×10^{13} Hz (21 μm) and 3.3×10^{13} Hz (9.1 μm) respectively. These correspond to different vibrational modes of the molecule. The detailed modelling of these absorption bands by the oscillator model will be discussed in Chapter 10.

The ultraviolet absorption in silica is caused by interband electronic transitions. SiO_2 has a fundamental band gap of about 10 eV, and interband transitions are possible whenever the photon energy exceeds this value. Hence we observe an absorption threshold in the ultraviolet at 2×10^{15} Hz (150 nm). The interband absorption peaks at around 3×10^{15} Hz with an extremely high absorption coefficient of $\sim 10^8\,\text{m}^{-1}$, and then gradually falls off to higher frequency. Subsidiary peaks are observed at $\sim 3 \times 10^{16}$ Hz and 1.3×10^{17} Hz. These are caused by transitions of the inner core electrons of the silicon and oxygen atoms. The fact that the electronic absorption consists of a continuous band rather than a discrete line makes it hard to model accurately as a Lorentz oscillator. We will discuss the quantum theory of the interband absorption in Chapter 3.

The refractive index of glass has resonances in the infrared and the ultraviolet which correspond to the interband and vibrational absorption. In the far infrared region below the vibrational resonance, the refractive index is ~ 2, while in the hard ultraviolet and X-ray region it approaches unity. In the transparency region between the vibrational and interband absorption, the refractive index has a value of ~ 1.5. Closer inspection of Fig. 2.7 shows that the refractive index actually increases with frequency in this transparency region, rising from a value of 1.40 at 8×10^{13} Hz (3.5 μm) to 1.55 at 1.5×10^{15} Hz (200 nm). This dispersion originates from the low frequency wings of the ultraviolet absorption and the high frequency wings of the infrared absorption, and will be discussed in more detail in Section 2.3 below.

The data in Fig. 2.7 show that the refractive index falls below unity at a number of frequencies. This implies that the phase velocity of the light is greater than c, which might seem to imply a contradiction with relativity. However, this overlooks the fact that a signal must be transmitted as a wave packet rather than as a monochromatic wave. In a dispersive medium, a wave packet will propagate at the **group velocity** v_g given by:

$$v_g = \frac{d\omega}{dk}, \tag{2.25}$$

rather than at the phase velocity $v = \omega/k = c/n$. The relationship between v_g and v is:

$$v_g = v\left(1 - \frac{k}{n}\frac{dn}{dk}\right). \tag{2.26}$$

The derivation of this result is left as an exercise to the reader. (See Exercise 2.7.) We will see in Section 2.3 that dn/dk is positive in most materials at optical frequencies. This then implies that v_g is always less than v, and if we were to try to transmit a signal in a spectral region where $v > c$, we

It is apparent from Fig. 2.6 that dn/dk will be negative at some frequencies close to one of the resonance lines. Equation 2.26 then implies that $v_g > v$, and so we could again run into a problem with relativity. However, the medium is highly absorbing in these frequency regions, and this means that the signal travels with yet another velocity called the signal velocity. This is always less than c.

would always find that v_g is less than c. The proof of this for a simple Lorentz oscillator is considered in Exercise 2.8.

2.2.4 Local field corrections

The calculation of the dielectric constant given in eqn 2.24 is valid in a rarefied gas with a low density of atoms. However, in a dense optical medium such as a solid, there is another factor that we must consider. The individual atomic dipoles respond to the **local field** that they experience. This may not necessarily be the same as the external field, because the dipoles themselves generate electric fields which will be felt by all the other dipoles. The actual local field experienced by an atom therefore takes the form:

$$\mathcal{E}_{\text{local}} = \mathcal{E} + \mathcal{E}_{\text{other dipoles}}\,, \tag{2.27}$$

where $\mathcal{E}$ and $\mathcal{E}_{\text{other dipoles}}$ represent the fields due to the external field and the other dipoles respectively. We should have been using $\mathcal{E}_{\text{local}}$ instead of $\mathcal{E}$ all along throughout the calculation given in Sections 2.2.1 and 2.2.2.

The calculation of the correction field due to the other dipoles in the medium is actually a rather complicated one. An approximate solution due to Lorentz can be derived if we assume that all the dipoles are parallel to the applied field and are arranged on a cubic lattice. The calculation works by separating the contribution from the nearby dipoles and that from the rest of the sample, as indicated in Fig. 2.8. The division is effected by an imaginary spherical surface with a radius large enough to make it sensible to average the material outside it. The problem is then reduced to summing the field of the dipoles inside the sphere at the one in the middle, and then calculating the effect of a uniformly polarized dielectric outside the sphere. The final result is:

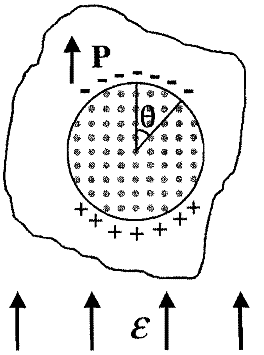

Fig. 2.8 Model used to calculate the local field by the Lorentz correction. An imaginary spherical surface drawn around a particular atom divides the medium into nearby dipoles and distant dipoles. The field at the centre of the sphere due to the nearby dipoles is summed exactly, while the field due to the distant dipoles is calculated by treating the material outside the sphere as a uniformly polarized dielectric.

$$\mathcal{E}_{\text{other dipoles}} = \frac{\mathbf{P}}{3\epsilon_0}\,, \tag{2.28}$$

where $\mathbf{P}$ is the polarization of the dielectric outside the sphere. The derivation of this result is the subject of Exercise 2.9. By using the result of eqn 2.28 in eqn 2.27 we find that:

$$\mathcal{E}_{\text{local}} = \mathcal{E} + \frac{\mathbf{P}}{3\epsilon_0}\,. \tag{2.29}$$

The macroscopic polarization $\mathbf{P}$ will be given by

$$\mathbf{P} = N\epsilon_0\chi_{\text{a}}\mathcal{E}_{\text{local}} \tag{2.30}$$

where χ_{a} is the electric susceptibility per atom. χ_{a} is defined by:

$$\mathbf{p} = \epsilon_0\chi_{\text{a}}\mathcal{E}_{\text{local}}\,, \tag{2.31}$$

$\mathbf{p}$ being the induced dipole moment per atom. This is analogous to the usual definition of the macroscopic susceptibility given in eqn A.1, except that it is now applied to individual atoms interacting with the local field. We can see from eqn 2.10 that χ_{a} is given by

$$\chi_{\text{a}} = \frac{e^2}{\epsilon_0 m_0}\frac{1}{\left(\omega_0^2 - \omega^2 - i\gamma\omega\right)}\,, \tag{2.32}$$

if there is just a single resonance. This is modified to

$$\chi_{\mathrm{a}} = \frac{e^2}{\epsilon_0 m_0} \sum_j \frac{f_j}{\left(\omega_j^2 - \omega^2 - i\gamma_j \omega\right)}, \tag{2.33}$$

if there are multiple resonances (cf. eqn 2.24).

We can combine eqns 2.29 and 2.30 with eqns 2.11 and 2.13 by writing

$$\mathbf{P} = N\epsilon_0 \chi_{\mathrm{a}} \left(\boldsymbol{\mathcal{E}} + \frac{\mathbf{P}}{3\epsilon_0} \right) = (\epsilon_{\mathrm{r}} - 1)\epsilon_0 \boldsymbol{\mathcal{E}} \,. \tag{2.34}$$

We put all this together to find that:

$$\frac{\epsilon_{\mathrm{r}} - 1}{\epsilon_{\mathrm{r}} + 2} = \frac{N\chi_{\mathrm{a}}}{3} \,. \tag{2.35}$$

This result is known as the **Clausius–Mossotti relationship**. The relationship works well in gases and liquids. It is also valid for those crystals in which the Lorentz correction given in eqn 2.29 gives an accurate account of the local field effects, namely cubic crystals.

2.2.5 The Kramers–Kronig relationships

The discussion of the dipole oscillator shows that the refractive index and the absorption coefficient are not independent parameters but are related to each other. This is a consequence of the fact that they are derived from the real and imaginary parts of a single parameter, namely the complex refractive index. If we invoke the law of causality (that an effect may not precede its cause) and apply complex number analysis, we can derive general relationships between the real and imaginary parts of the refractive index. These are known as the **Kramers–Kronig** relationships and may be stated as follows:

$$n(\omega) = 1 + \frac{1}{\pi} \,\mathsf{P} \int_{-\infty}^{\infty} \frac{\kappa(\omega')}{\omega' - \omega}\, d\omega' \tag{2.36}$$

$$\kappa(\omega) = -\frac{1}{\pi} \,\mathsf{P} \int_{-\infty}^{\infty} \frac{n(\omega') - 1}{\omega' - \omega}\, d\omega', \tag{2.37}$$

where P indicates that we take the principal part of the integral.

The Kramers–Kronig relationships allow us to calculate n from κ, and *vice versa*. This can be very useful in practice, because it would allow us, for example, to measure the frequency dependence of the optical absorption and then calculate the dispersion without needing to make a separate measurement of n.

2.3 Dispersion

Figure 2.9 plots the refractive index data from Fig. 2.7 in more detail. The data show that the refractive index increases with frequency in the near infrared and visible spectral regions. We have seen in Section 2.2.3 that this dispersion originates mainly from the interband absorption in the ultraviolet. At visible

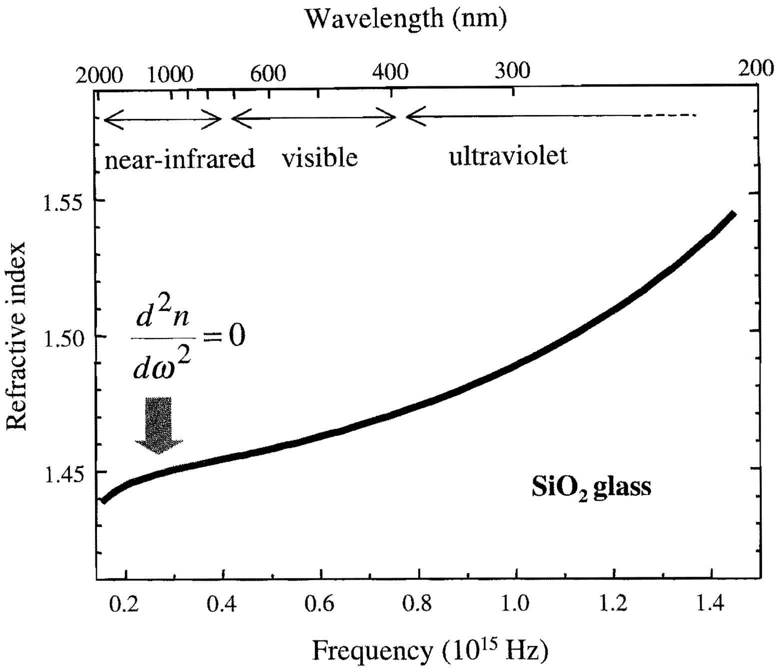

Fig. 2.9 Refractive index of SiO_2 glass in the near infrared, visible and ultraviolet spectral regions. After [1].

frequencies the absorption from these transitions is negligible and the glass is transparent. However, the ultraviolet absorption still affects the refractive index through the extreme wings of the Lorentzian line. In the near infrared, the dispersion is also affected by the high frequency wings of the vibrational absorption at lower frequency.

A material in which the refractive index increases with frequency is said to have **normal** dispersion, while one in which the contrary occurs is said to have **anomalous** dispersion. A number of empirical formulae to describe the normal dispersion of glasses have been developed over the years. (See Exercise 2.12.)

The use of the words 'normal' and 'anomalous' is somewhat misleading here. The dipole oscillator model shows us that all materials have anomalous dispersion at some frequencies. The phraseology was adopted before measurements of the refractive index had been made over a wide frequency range and the origin of dispersion had been properly understood.

The dispersion of the refractive index of glasses such as silica can be used to separate different wavelengths of light with a prism, as shown in Fig. 2.10. The blue light is refracted more because of the higher index of refraction, and is therefore deviated through a larger angle by the prism. (See Exercise 2.13.) This effect is used in prism spectrometers.

One of the effects of dispersion is that light of different frequencies takes a different amount of time to propagate through a material. (See Exercise 1.11, for example.) A pulse of light of duration t_p must necessarily contain a spread of frequencies given approximately by

$$\Delta\nu \approx \frac{1}{t_\mathrm{p}} \qquad (2.38)$$

in order to satisfy the 'uncertainty principle' $\Delta\nu\Delta t \sim 1$. Dispersion will therefore cause the pulse to broaden in time as it propagates through the medium. This can become a serious problem when attempting to transmit very short pulses through a long length of an optical material, for example in a high speed optical fibre telecommunications system.

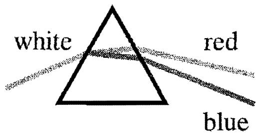

Fig. 2.10 Separation of white light into different colours by dispersion in a glass prism.

We mentioned in Section 2.2.3 that a pulse of light travels with the group velocity v_g. The important parameter for pulse spreading due to dispersion is therefore the **group velocity dispersion** (GVD) (see Exercise 2.14):

$$\mathrm{GVD} = \frac{d^2\omega}{dk^2} \propto \frac{d^2n}{d\omega^2} \propto \frac{d^2n}{d\lambda^2}\,. \tag{2.39}$$

The Lorentz model indicates that the GVD is positive below an absorption line and negative above it. Applying this to the data in Fig. 2.9, we see negative GVD in the infrared due to the vibrational absorption and positive GVD in the visible due to the interband absorption in the ultraviolet. These two effects cancel at a wavelength in the near infrared which is identified in Fig. 2.9. This region of zero GVD occurs around 1.3 μm in silica optical fibres. Short pulses can be transmitted down the fibre with negligible temporal broadening at this wavelength, and so it is one of the preferred wavelengths for optical fibre communication systems.

2.4 Optical anisotropy: birefringence

The atoms in a solid are locked into a crystalline lattice with well defined axes. In general, we cannot assume that the optical properties along the different crystalline axes are equivalent. For example, the separation of the atoms might not be the same in all directions. This would lead to different vibrational frequencies, and hence a change in the refractive index between the relevant directions. This optical anisotropy contrasts with gases and liquids which are isotropic because the atoms have no preferred directions in the absence of external perturbations such as applied magnetic or electric fields.

Optical anisotropy gives rise to the phenomenon of **birefringence**. We can describe the properties of a birefringent crystal by generalizing the relationship between the polarization and the applied electric field. If the electric field is applied along an arbitrary direction relative to the crystalline axes, we must write a tensor equation to relate **P** to $\boldsymbol{\mathcal{E}}$:

$$\mathbf{P} = \epsilon_0 \chi \boldsymbol{\mathcal{E}} \tag{2.40}$$

where χ represents the susceptibility tensor. Written explicitly in terms of the components, we have:

$$\begin{pmatrix} P_x \\ P_y \\ P_z \end{pmatrix} = \epsilon_0 \begin{pmatrix} \chi_{11} & \chi_{12} & \chi_{13} \\ \chi_{21} & \chi_{22} & \chi_{23} \\ \chi_{31} & \chi_{32} & \chi_{33} \end{pmatrix} \begin{pmatrix} \mathcal{E}_x \\ \mathcal{E}_y \\ \mathcal{E}_z \end{pmatrix}. \tag{2.41}$$

We can simplify this by choosing the cartesian coordinates x, y, and z to correspond to the principal crystalline axes. In this case, the off-diagonal components are zero, and the susceptibility tensor takes the form:

$$\chi = \begin{pmatrix} \chi_{11} & 0 & 0 \\ 0 & \chi_{22} & 0 \\ 0 & 0 & \chi_{33} \end{pmatrix}. \tag{2.42}$$

The relationships between the components are determined by the crystal symmetry.

Equation 2.40 should be contrasted with the usual *scalar* relationship between **P** and $\boldsymbol{\mathcal{E}}$ namely (cf. eqn A.1):

$$\mathbf{P} = \epsilon_0 \chi \boldsymbol{\mathcal{E}}\,,$$

which only applies to isotropic materials.

Table 2.1 Refractive indices of some common uniaxial crystals at 589.3 nm. After [2].

Crystal	Chemical structure	Symmetry class	type	n_o	n_e
Ice	H_2O	trigonal	positive	1.309	1.313
Quartz	SiO_2	trigonal	positive	1.544	1.553
Beryl	$Be_3Al_2(SiO_3)_6$	hexagonal	negative	1.581	1.575
Sodium nitrate	$NaNO_3$	trigonal	negative	1.584	1.336
Calcite	$CaCO_3$	trigonal	negative	1.658	1.486
Tourmaline	complex silicate	trigonal	negative	1.669	1.638
Sapphire	Al_2O_3	trigonal	negative	1.768	1.760
Zircon	$ZrSiO_4$	tetragonal	positive	1.923	1.968
Rutile	TiO_2	tetragonal	positive	2.616	2.903

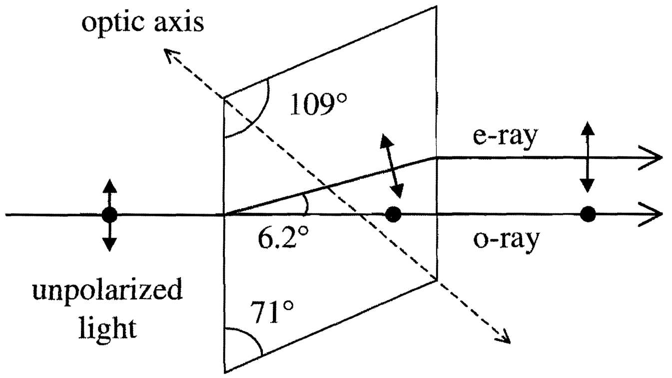

Fig. 2.11 Double refraction in a natural calcite crystal. The shape of the crystal and the orientation of the optic axis is determined by the cleavage planes of calcite. An unpolarized incident light ray is split into two spatially separated orthogonally polarized rays. The • symbol for the o-ray indicates that it is polarized with its field pointing out of the page.

- In cubic crystals, the x, y and z axes are indistinguishable. They therefore have $\chi_{11} = \chi_{22} = \chi_{33}$, and their optical properties are isotropic.
- Crystals with tetragonal, hexagonal or trigonal (rhombohedral) symmetry are called **uniaxial** crystals. These crystals possess a single **optic axis**, which is usually taken as the z axis. In hexagonal crystals, for example, the optic axis is defined by the direction normal to the plane of the hexagons. The optical properties are the same along the x and y directions, but not along the z direction. This implies that $\chi_{11} = \chi_{22} \neq \chi_{33}$. Some examples of uniaxial crystals are listed in Table 2.1.
- Crystals with orthorhombic, monoclinic or triclinic symmetry are called **biaxial** crystals. They have two optic axes, and all three diagonal components of the susceptibility tensor are different. Mica is an important example of a biaxial crystal, since it is widely used for making optical wave plates.

Crystals with cubic symmetry are only isotropic as regards their *linear* optical properties. We will see in Chapter 11 that cubic crystals can actually have anisotropic *nonlinear* optical properties.

One very striking demonstration of optical anisotropy is the phenomenon of **double refraction**. In this effect an unpolarized light ray is separated into two rays which emerge displaced from each other, as shown in Fig. 2.11. These two rays are called 'ordinary' and 'extraordinary', and are orthogonally polarized to each other.

The phenomenon of double refraction can be explained by assuming that the crystal has different refractive indices for the orthogonal polarizations of the ordinary and extraordinary rays. These two refractive indices are usually labelled n_o and n_e respectively. Consider the propagation of a beam of unpo-

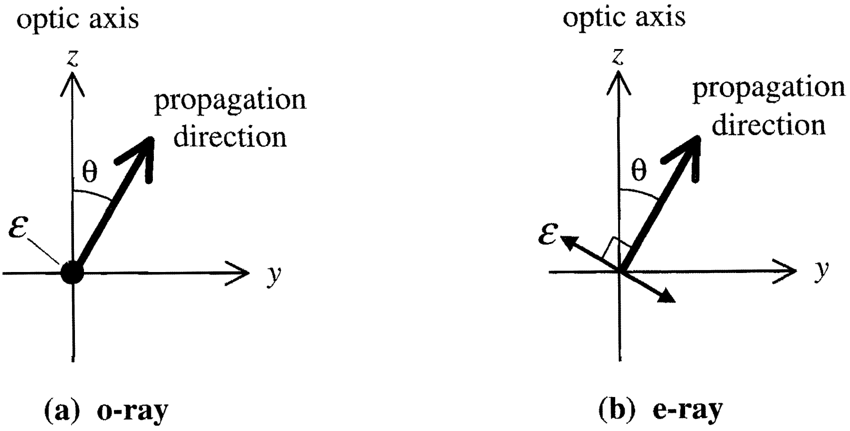

(a) o-ray **(b) e-ray**

Fig. 2.12 Electric field vector of ray propagating in a uniaxial crystal with its optic axis along the z direction. The ray makes an angle of θ with respect to the optic axis. The x and y axes are chosen so that the beam is propagating in the y, z plane. The polarization can be resolved into: (a) a component along the x axis and (b) a component at an angle of $90° - \theta$ to the optic axis. (a) is the o-ray and (b) is the e-ray.

larized light which enters a uniaxial crystal at an angle θ to the optic axis, which is taken to lie along the z axis. The optical properties are isotropic in the x, y plane, and so we can choose the axes so that the beam is propagating in the y, z plane without loss of generality, as shown in Fig. 2.12. This allows us to split the polarization of the light into two orthogonal components, one of which is polarized along the x axis, and the other polarized at an angle of $(90° - \theta)$ to the optic axis. The former is the o(rdinary)-ray, and the latter is the e(xtraordinary)-ray. Now the refractive index will be different for light which is polarized along the z axis or in the x, y plane. Therefore the o-ray experiences a different refractive index to the e-ray, and will thus be refracted differently: hence double refraction. On the other hand, if the beam propagates along the optic axis so that $\theta = 0$, the $\boldsymbol{\mathcal{E}}$-vector of the light will always fall in the x, y plane. In this case, no double refraction will be observed because the x and y directions are equivalent and there is no e-ray.

Double refraction was first observed in natural uniaxial crystals such as calcite ('Iceland Spar') and quartz. Table 2.1 lists the refractive indices for the o- and e-rays of calcite and quartz, together with those of several other uniaxial crystals. The birefringent crystals are classified as being either positive or negative depending on whether n_e is greater or smaller than n_o.

Further discussion of the detailed effects of birefringence can be found in most optics textbooks. The purpose of introducing birefringence here is to give an example of how the phenomenon of optical anisotropy arises from the underlying symmetry of the crystal structure. This is a very standard example of an optical effect that occurs in crystalline solids and is not found in gases or liquids.

Example 2.2

The optic axis of a uniaxial crystal lies along the z axis. The refractive index for light polarized in the z direction is n_e, while that for light polarized in the x, y plane is n_o. Write down the dielectric constant tensor defined through the tensor relationship

$$\mathbf{D} = \epsilon_0 \epsilon_r \boldsymbol{\mathcal{E}} \, .$$

Solution

We make use of eqns 2.11 and 2.40 to write:

$$\begin{aligned}\mathbf{D} &= \epsilon_0 \boldsymbol{\mathcal{E}} + \mathbf{P} \\ &= \epsilon_0 \boldsymbol{\mathcal{E}} + \epsilon_0 \boldsymbol{\chi} \boldsymbol{\mathcal{E}} \\ &= \epsilon_0 (\mathbf{1} + \boldsymbol{\chi}) \boldsymbol{\mathcal{E}} \equiv \epsilon_0 \boldsymbol{\epsilon}_\mathbf{r} \boldsymbol{\mathcal{E}} \, . \end{aligned} \tag{2.43}$$

Hence we see that:

$$\boldsymbol{\epsilon}_\mathbf{r} = \mathbf{1} + \boldsymbol{\chi} \tag{2.44}$$

The susceptibility tensor is given by eqn 2.42, and hence the dielectric constant tensor will take the form:

$$\boldsymbol{\epsilon}_\mathbf{r} = \begin{pmatrix} 1+\chi_{11} & 0 & 0 \\ 0 & 1+\chi_{22} & 0 \\ 0 & 0 & 1+\chi_{33} \end{pmatrix} . \tag{2.45}$$

In a uniaxial crystal with the optic axis along the z direction, we must have $\chi_{11} = \chi_{22} \neq \chi_{33}$.

We now further assume that the crystal is transparent, so that the dielectric constant is just equal to the square of the refractive index (cf. eqns 1.24 and 1.25 with $\kappa = 0$). If we had a linearly polarized light beam with the electric field directed along the x or y directions, we would measure a refractive index of n_o. This tells us that

$$1 + \chi_{11} = 1 + \chi_{22} = n_\mathrm{o}^2 \, .$$

On the other hand, if $\boldsymbol{\mathcal{E}}$ is along the z axis, we would measure a refractive index of n_e, which implies that

$$1 + \chi_{33} = n_\mathrm{e}^2 \, .$$

Therefore the dielectric constant tensor must be:

$$\boldsymbol{\epsilon}_\mathbf{r} = \begin{pmatrix} n_\mathrm{o}^2 & 0 & 0 \\ 0 & n_\mathrm{o}^2 & 0 \\ 0 & 0 & n_\mathrm{e}^2 \end{pmatrix} . \tag{2.46}$$

Chapter summary

- The classical model of a solid treats the atoms and molecules as oscillating electric dipoles with characteristic resonant frequencies. The resonances due to the bound electrons occur in the near infrared, visible and ultraviolet spectral regions (10^{14}–10^{15} Hz), while those associated with vibrations occur in the infrared (10^{12}–10^{13} Hz). Free electrons can be treated in the dipole oscillator model by assuming that the natural resonant frequency is 0.

- The medium absorbs light when the frequency coincides with one of its resonant frequencies. In non-resonant conditions, the medium is transparent, but the velocity of light is reduced by multiple coherent elastic scattering.
- The absorption coefficient of an individual dipole oscillator has a Lorentzian line shape (cf. eqn 2.21). The spectral width of the absorption line is equal to the damping constant γ. The peak absorption is proportional to $1/\gamma$.
- The refractive index of a dipole oscillator increases as the frequency approaches the resonant frequency, then drops sharply in the absorbing region, and then increases again at higher frequencies. The off-resonant refractive index decreases each time we go through an absorption line.
- The dielectric constant of a medium with multiple resonant frequencies is given by eqn 2.24. The refractive index and absorption coefficient can be calculated from the real and imaginary parts of ϵ_r.
- The dipole oscillator model demonstrates that the absorption and refraction of an optical medium are fundamentally related to each other. This interrelationship is made explicit through the Kramers–Kronig formulae.
- Dispersion in the refractive index originates from the wings of the resonances at transition frequencies. The dispersion is called normal when the refractive index increases with frequency. Group velocity dispersion causes temporal broadening of short pulses.
- Optical anisotropy leads to birefringence. The anisotropy is described through the electric susceptibility tensor or the dielectric constant tensor.

Further reading

The subject matter of this chapter is covered, to a greater or lesser extent, in most electromagnetism and optics textbooks. See, for example: Bleaney and Bleaney (1976), Born and Wolf (1999), Hecht (1998) or Klein and Furtak (1986).

An excellent collection of optical data on a wide range of solid state materials can be found in Palik (1985).

For a fuller description of birefringence, see: Hecht (1998), Born and Wolf (1999) or Klein and Furtak (1986).

References

[1] Palik, E.D. (1985). *Handbook of the optical constants of solids*. Academic Press, San Diego.

[2] Driscoll, W.G. and Vaughan, W. (1978). *Handbook of optics*. McGraw-Hill, New York.

Exercises

(2.1) Write down the equations of motion for the frictionless displacements x_1 and x_2 of two masses, m_1 and m_2, connected together by a light spring with a spring constant K_{s}. Hence show that the angular frequency for small oscillations is equal to $(K_{\mathrm{s}}/\mu)^{\frac{1}{2}}$ where $\mu^{-1} = m_1^{-1} + m_2^{-1}$.

(2.2) A damped oscillator with mass m, natural frequency ω_0, and damping constant γ is being driven by a force of amplitude F_0 and frequency ω. The equation of motion for the displacement x of the oscillator is:

$$m\frac{d^2x}{dt^2} + m\gamma\frac{dx}{dt} + m\omega_0^2 x = F_0 \cos\omega t\,.$$

What is the phase of x relative to the phase of the driving force ?

(2.3) A sapphire crystal doped with titanium absorbs strongly around 500 nm. Calculate the difference in the refractive index of the doped crystal above and below the 500 nm absorption band if the density of absorbing atoms is $1 \times 10^{25}\,\mathrm{m}^{-3}$. The refractive index of undoped sapphire is 1.77.

(2.4) The laser crystal $\mathrm{Ni}^{2+}{:}\mathrm{MgF}_2$ has a broad absorption band in the blue which peaks at 405 nm and has a full width at half maximum of 8.2×10^{13} Hz. The oscillator strength of the transition is 9×10^{-5}. Estimate the maximum absorption coefficient in a crystal with $2\times10^{26}\mathrm{m}^{-3}$ absorbing atoms per unit volume. The refractive index of the crystal is 1.39.

(2.5) Show that the absorption coefficient of a Lorentz oscillator at the line centre does not depend on the value of ω_0.

(2.6) Figure 2.13 shows the refractive index of NaCl in the infrared spectral region. The data can be modelled approximately by assuming that the resonance feature is caused by the vibrations of the completely ionic $\mathrm{Na}^+\mathrm{Cl}^-$ molecules. The atomic weights of sodium and chlorine are 23 and 35.5 respectively. Use the data to estimate:

- (i) The static dielectric constant of NaCl.
- (ii) The natural oscillation frequency of the vibrations.
- (iii) The restoring force for a unit displacement of the oscillator.
- (iv) The density of NaCl molecules per unit volume.
- (v) The damping constant γ for the vibrations.
- (vi) The peak absorption coefficient.

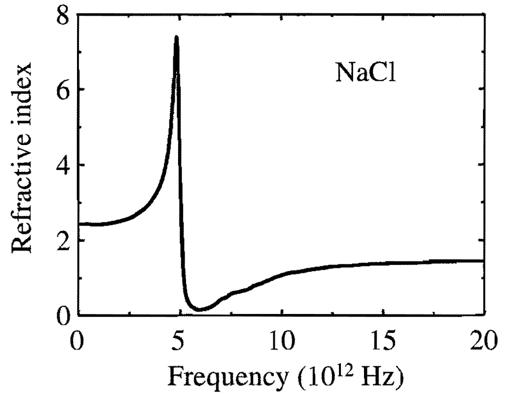

Fig. 2.13 Infrared refractive index of NaCl. After [1].

(2.7) Derive eqn 2.26.

(2.8)* Consider a simple Lorentz oscillator with a single undamped resonance. The dielectric constant will be given by eqn 2.14 with χ and γ both zero. This gives:

$$\epsilon_{\mathrm{r}}(\omega) = 1 + \frac{Ne^2}{\epsilon_0 m_0}\frac{1}{\left(\omega_0^2 - \omega^2\right)}\,.$$

Prove that the group velocity is always less than c.

(2.9)* Consider a dielectric sample placed in a uniform electric field pointing in the z direction as shown in Fig. 2.8. Assume that the atoms are arranged on a cubic lattice and the dipoles are all pointing along the external field direction.

- (i) Let us first consider the field generated by the dipoles within the spherical surface. By using the standard formula for the electric field generated by an electric dipole, show that the field at the centre of the sphere is given by

  $$\mathcal{E}_{\mathrm{sphere}} = \frac{1}{4\pi\epsilon_0}\sum_j p_j \frac{3z_j^2 - r_j^2}{r_j^5}$$

  where the summation runs over all the dipoles within the surface except the one at the centre, and p_j is the dipole moment of the atom at the jth lattice site.
- (ii) Show that $\mathcal{E}_{\mathrm{sphere}} = 0$ in a homogenous medium where all the p_j's are the same.

---

* Exercises marked with an asterisk are more challenging.

(iii) Now consider the uniformly polarized dielectric material outside the spherical hole. Let **P** be the macroscopic polarization of the medium, which is assumed to be parallel to the external field. Show that the surface charge density on the sphere at an angle θ from the z axis is equal to $-P\cos\theta$. Hence show that the material outside the spherical surface generates a field at the centre of the sphere equal to $-\mathbf{P}/3\epsilon_0$.

(2.10) Under what conditions does the Clausius–Mossotti relationship given by eqn 2.35 reduce to the usual relationship between the dielectric constant and the electric susceptibility given in eqn A.4 ?

(2.11) The relative dielectric constant of N_2 gas at standard temperature and pressure is 1.000588. Calculate χ_a for the N_2 molecule. Show that the electric field strength required to generate a dipole equivalent to displacing the electron by 1 Å (10^{-10} m) is of a similar magnitude to the electric field between a proton and an electron separated by the same distance.

(2.12) (a) Sellmeier derived the following equation for the wavelength dependence of the refractive index in 1871:

$$n^2 = 1 + \sum_j \frac{A_j\lambda^2}{\left(\lambda^2 - \lambda_j^2\right)}\,.$$

Show that this equation is equivalent to eqn 2.24 in regions of transparency far from any absorption lines. State the values of A_j and λ_j.

(b) Assume that the dispersion is dominated by the closest resonance, so that we only need to include one term (say the one with $j = 1$) in the summation of Sellmeier's equation. Assume that λ_1^2/λ^2 is small, and expand Sellmeier's equation to derive the earlier dispersion formula determined empirically by Cauchy:

$$n = C_1 + \frac{C_2}{\lambda^2} + \frac{C_3}{\lambda^4} + \cdots$$

State the values of C_1, C_2 and C_3 in terms of A_1 and λ_1.

(2.13) The refractive index of crown glass is 1.5553 at 402.6 nm and 1.5352 at 706.5 nm.

(i) Determine the coefficients C_1 and C_2 in Cauchy's formula given in the previous question, on the assumption that the term in C_3 is negligible.

(ii) Estimate the refractive index for blue light at 450 nm and for red light at 650 nm.

(iii) White light strikes a crown glass prism with an apex angle of 60°, as shown in Fig. 2.10. The angle of incidence with the first surface is 45°. Calculate the difference in the angle between the light at 450 nm and 650 nm at the exit surface of the prism.

(2.14) Show that the temporal broadening of a short pulse by a dispersive medium of length L is given approximately by:

$$\Delta\tau = \frac{L}{c}\left(\lambda^2\frac{d^2n}{d\lambda^2}\right)\frac{\Delta\lambda}{\lambda}$$

where λ is the vacuum wavelength and $\Delta\lambda$ is the spectral width of the pulse. Estimate $\Delta\tau$ for an ultrashort laser pulse with a temporal width of 1 ps in 1 m of optical fibre at 1550 nm, where $\lambda^2 d^2n/d\lambda^2 = -0.01$.

(2.15) Consider the propagation of a wave with polarization vector components (x, y, z), where $x^2+y^2+z^2 = 1$, in a birefringent medium. The dielectric constant experienced by the wave is conveniently described by the index ellipsoid:

$$\frac{x^2}{\epsilon_{11}/\epsilon_0} + \frac{y^2}{\epsilon_{22}/\epsilon_0} + \frac{z^2}{\epsilon_{33}/\epsilon_0} = 1\,,$$

where the ϵ_{ij} are the components of the dielectric constant tensor defined in eqn 2.45. The use of the index ellipsoid can be justified by considering the direction of the energy flow through the crystal: see Born and Wolf (1999). Use the index ellipsoid to show that the refractive index for the e-ray propagating at an angle θ to the optic axis of a uniaxial crystal as shown in Fig. 2.12(b) is given by:

$$\frac{1}{n(\theta)^2} = \frac{\sin^2\theta}{n_e^2} + \frac{\cos^2\theta}{n_o^2}\,,$$

where n_e and n_o are defined in Example 2.2.

(2.16) A uniaxial birefringent crystal made from quartz has $n_o = 1.5443$ and $n_e = 1.5534$. A wave plate is made by cutting the crystal so that the optic axis is parallel to the surfaces of the plate. The crystal will function as a quarter wave plate if the phase difference between the o- and e-rays is 90°, turning light polarized at 45° to the optic axis into circularly polarized light. Calculate the thickness of the crystal if it behaves as a quarter wave plate at 500 nm.

(2.17) Look up the crystal structure of the following materials to determine whether they are birefringent or not: (a) NaCl, (b) diamond, (c) graphite (in the infrared, where it transmits), (d) ZnS (wurtzite structure), (e) ZnS (zinc blende structure), (f) solid argon at 4 K, (g) sulphur. Specify which, if any, of the birefringent materials are biaxial.

Appendix A

Electromagnetism in dielectrics

This appendix summarizes the principal results of electromagnetism that are used throughout the book. It is hoped that the reader will be familiar with this material. The main purpose of the appendix is to collect together the equations in a concise form for quick reference, and also to define the notation. SI units are used throughout. A short bibliography of suitable supplementary texts is given under Further Reading.

A.1 Electromagnetic fields and Maxwell's equations

The response of a dielectric material to an external electric field is characterized by three macroscopic vectors:

- the **electric field strength** $\boldsymbol{\mathcal{E}}$;
- the **polarization** $\mathbf{P}$;
- the **electric displacement** $\mathbf{D}$.

The microscopic response of the material is determined primarily by the polarization. For this reason, the first task in all the examples treated by electromagnetism in this book is to calculate $\mathbf{P}$. The dielectric constant ϵ_r is then determined from $\mathbf{P}$, and the optical properties are deduced from ϵ_r.

The polarization is defined as the net dipole moment per unit volume. The application of a field produces a polarization by the forces exerted on the positive and negative charges of the atoms that are contained within the medium. If the atoms have permanent dipole moments, the field will apply a torque to these randomly orientated dipoles and tend to align them along the field direction. If there are no permanent dipoles, the field will push the positive and negative charges in opposite directions and induce a dipole parallel to the field. In either case, the end result is the same: the application of the field tends to produce many microscopic dipoles aligned parallel to the direction of the external field. This generates a net dipole moment within the dielectric, and hence a polarization.

The microscopic dipoles will all tend to align along the field direction, and so the polarization vector will be parallel to $\boldsymbol{\mathcal{E}}$. This allows us to write:

$$\mathbf{P} = \epsilon_0 \chi \boldsymbol{\mathcal{E}}, \tag{A.1}$$

where ϵ_0 is the **electric permittivity** of free space and χ is the **electric susceptibility** of the medium.

$\epsilon_0 = 8.854 \times 10^{-12}\,\mathrm{Fm}^{-1}$ in SI units.

Equation A.1 makes two assumptions that need a brief word of explanation.

(1) We have assumed that the medium is isotropic, even though we know that some materials are anisotropic. In particular, anisotropic crystals have preferred non-equivalent axes, and **P** will not necessarily be parallel to $\boldsymbol{\mathcal{E}}$.
(2) We have assumed that **P** varies linearly with $\boldsymbol{\mathcal{E}}$. This will not always be the case. In particular, if the optical intensity is very large, we can enter the realm of nonlinear optics, in which eqn A.1 is not valid.

Both of these qualifications introduce unnecessary complications at this stage, and are not considered further in this appendix. A discussion of how to treat non-isotropic materials may be found in Section 2.4, while nonlinear optics is the subject of Chapter 11.

The electric displacement **D** of the medium is related to the electric field $\boldsymbol{\mathcal{E}}$ and polarization **P** through:

$$\mathbf{D} = \epsilon_0 \boldsymbol{\mathcal{E}} + \mathbf{P}. \tag{A.2}$$

This may be considered to be the definition of **D**. By combining eqns A.1 and A.2, we can write:

$$\mathbf{D} = \epsilon_0 \epsilon_r \boldsymbol{\mathcal{E}}, \tag{A.3}$$

where

$$\epsilon_r = 1 + \chi\,. \tag{A.4}$$

ϵ_r is the **relative dielectric constant** of the medium, and is an extremely important parameter in the understanding of the propagation of light through dielectrics.

In electrostatic problems we are frequently interested in calculating the spatial dependence of electric field, and hence the electric potential V, from the free charge density ϱ. This calculation can be performed by using the Poisson equation:

$$\nabla^2 V = -\frac{\varrho}{\epsilon_r \epsilon_0}. \tag{A.5}$$

Poisson's equation is derived from Gauss's law of electrostatics:

$$\nabla \cdot \boldsymbol{\mathcal{E}} = \frac{\varrho}{\epsilon_r \epsilon_0}. \tag{A.6}$$

We recall that the electric field strength is the gradient of the potential:

$$\boldsymbol{\mathcal{E}} = -\nabla V. \tag{A.7}$$

Equation A.5 follows directly by substituting for $\boldsymbol{\mathcal{E}}$ in eqn A.6 using eqn A.7. Once we know V, we can then calculate $\boldsymbol{\mathcal{E}}$ from eqn A.7. This approach is also useful when we are treating devices in which the potential across the device is fixed by an external voltage source.

The response of a material to external magnetic fields is treated in a similar way to the response of dielectrics to electric fields. The **magnetization** **M** of the medium is proportional to the **magnetic field strength** **H** through the **magnetic susceptibility** χ_M:

$$\mathbf{M} = \chi_M \mathbf{H}. \tag{A.8}$$

The **magnetic flux density** **B** is related to **H** and **M** through:

$$\begin{aligned}\mathbf{B} &= \mu_0(\mathbf{H}+\mathbf{M})\\ &= \mu_0(1+\chi_M)\mathbf{H}\\ &= \mu_0\mu_r\mathbf{H},\end{aligned} \tag{A.9}$$

where μ_0 is the magnetic permeability of the vacuum and $\mu_r = 1 + \chi_M$ is the **relative magnetic permeability** of the medium.

$\mu_0 = 4\pi \times 10^{-7}\mathrm{Hm}^{-1}$ in SI units.

The laws that describe the combined electric and magnetic response of a medium are summarized in **Maxwell's equations** of electromagnetism:

$$\nabla \cdot \mathbf{D} = \varrho \tag{A.10}$$

$$\nabla \cdot \mathbf{B} = 0 \tag{A.11}$$

$$\nabla \wedge \boldsymbol{\mathcal{E}} = -\frac{\partial \mathbf{B}}{\partial t} \tag{A.12}$$

$$\nabla \wedge \mathbf{H} = \mathbf{j} + \frac{\partial \mathbf{D}}{\partial t}, \tag{A.13}$$

where ϱ is the free charge density, and **j** is the current density. The first of these four equations is Gauss's law of electrostatics (eqn A.6) written in terms of **D** rather than $\boldsymbol{\mathcal{E}}$. The second is the equivalent of Gauss's law for magnetostatics with the assumption that free magnetic monopoles do not exist. The third equation combines the Faraday and Lenz laws of electromagnetic induction. The fourth is a statement of Ampere's law, with the second term on the right hand side to account for the displacement current.

The second Maxwell equation naturally leads to the concept of the **vector potential**. This is defined through the equation

$$\mathbf{B} = \nabla \wedge \mathbf{A}. \tag{A.14}$$

We see that the vector potential **A** automatically satisfies eqn A.11, because $\nabla \cdot (\nabla \wedge \mathbf{A}) = 0$ for all **A**. However, this definition does not define **A** uniquely. We can add any vector of the form $\nabla\varphi$ to **A** without changing **B**. This follows because

$$\nabla \wedge (\mathbf{A} + \nabla\varphi) = \nabla \wedge \mathbf{A} + \nabla \wedge (\nabla\varphi) = \nabla \wedge \mathbf{A}. \tag{A.15}$$

$\varphi(\mathbf{r})$ can be any scalar function of **r**. For this reason, we have to give an additional definition, which specifies the **gauge** in which we are working. The **Coulomb gauge** is defined by

$$\nabla \cdot \mathbf{A} = 0. \tag{A.16}$$

This gauge is a convenient one because it allows us to derive a simple relationship between $\boldsymbol{\mathcal{E}}$ and **A**. By substituting for **B** in the third Maxwell equation (eqn A.12) using eqn A.14, we see that:

$$\nabla \wedge \boldsymbol{\mathcal{E}} = -\frac{\partial}{\partial t}(\nabla \wedge \mathbf{A}) = \nabla\wedge \left(-\frac{\partial \mathbf{A}}{\partial t}\right). \tag{A.17}$$

The solution is

$$\boldsymbol{\mathcal{E}} = -\frac{\partial \mathbf{A}}{\partial t} + \text{constant}, \tag{A.18}$$

where the constant is any vector whose curl is zero. If the scalar potential is V, then we can combine eqn A.18 with eqn A.7 by writing

$$\boldsymbol{\mathcal{E}} = -\frac{\partial \mathbf{A}}{\partial t} - \nabla V\,. \tag{A.19}$$

This works because $\nabla \wedge \nabla V = 0$. By taking the divergence of eqn A.19, we can recover Poisson's equation (A.5) if we satisfy eqn A.16, that is, if we are in the Coulomb gauge. The more general definition of $\boldsymbol{\mathcal{E}}$ given in eqn A.19 reduces to eqn A.7 when the magnetic field does not vary with time, and to

$$\boldsymbol{\mathcal{E}} = -\frac{\partial \mathbf{A}}{\partial t} \tag{A.20}$$

when the static potential is constant throughout space. The vector potential in the Coulomb gauge is used in the semiclassical treatment of the interaction of light with atoms discussed in Section B.2 of Appendix B.

A.2 Electromagnetic waves

Maxwell was able to show that eqns A.10–A.13 were consistent with wave-like solutions in a medium with no free charges or currents. To see this we first simplify eqns A.12 and A.13 by setting $\mathbf{j} = 0$ and eliminating $\mathbf{B}$ and $\mathbf{D}$ using eqns A.3 and A.9. This gives:

$$\nabla \wedge \boldsymbol{\mathcal{E}} = -\mu_0\mu_r \frac{\partial \mathbf{H}}{\partial t}\,, \tag{A.21}$$

and

$$\nabla \wedge \mathbf{H} = \epsilon_0\epsilon_r \frac{\partial \boldsymbol{\mathcal{E}}}{\partial t}\,. \tag{A.22}$$

We then take the curl of eqn A.21 and eliminate $\nabla \wedge \mathbf{H}$ using eqn A.22. This gives:

$$\nabla \wedge (\nabla \wedge \boldsymbol{\mathcal{E}}) = -\,\mu_0\mu_r\epsilon_0\epsilon_r\,\frac{\partial^2 \boldsymbol{\mathcal{E}}}{\partial t^2}\,. \tag{A.23}$$

The left hand side can be simplified by using the vector identity

$$\nabla \wedge (\nabla \wedge \boldsymbol{\mathcal{E}}) = \nabla(\nabla \cdot \boldsymbol{\mathcal{E}}) - \nabla^2 \boldsymbol{\mathcal{E}}\,. \tag{A.24}$$

Equation A.6 with $\varrho = 0$ tells us that $\nabla \cdot \boldsymbol{\mathcal{E}} = 0$. Therefore we obtain the final result:

$$\nabla^2 \boldsymbol{\mathcal{E}} = \mu_0\mu_r\epsilon_0\epsilon_r\,\frac{\partial^2 \boldsymbol{\mathcal{E}}}{\partial t^2}\,. \tag{A.25}$$

Equation A.25 is of the same form as the wave equation:

$$\frac{\partial^2 y}{\partial x^2} = \frac{1}{v^2}\frac{\partial^2 y}{\partial t^2}, \tag{A.26}$$

where v is the velocity of the wave. We therefore identify eqn A.25 as describing electromagnetic waves with a phase velocity v given by

$$\frac{1}{v^2} = \mu_0\mu_r\epsilon_0\epsilon_r. \tag{A.27}$$

In free space $\epsilon_r = \mu_r = 1$ and the velocity of the wave is c, so we have:

$$c = \frac{1}{\sqrt{\mu_0 \epsilon_0}} = 2.998 \times 10^8 \text{ m s}^{-1}. \tag{A.28}$$

At the same time, we see from eqns A.27 and A.28 that the velocity in a medium is given by

$$v = \frac{1}{\sqrt{\epsilon_r \mu_r}} c\,. \tag{A.29}$$

We define the **refractive index** n of the medium as the ratio of the velocity of light in free space to the velocity in the medium:

$$n = \frac{c}{v}\,. \tag{A.30}$$

At optical frequencies we can set $\mu_r = 1$, and thus conclude:

$$n = \sqrt{\epsilon_r}. \tag{A.31}$$

This allows us to relate the propagation constants of electromagnetic waves in a medium to the dielectric constant.

The solutions to eqn A.25 are of the form

$$\boldsymbol{\mathcal{E}}(z, t) = \boldsymbol{\mathcal{E}}_0 \, \mathrm{e}^{i(kz - \omega t)}\,, \tag{A.32}$$

where $\boldsymbol{\mathcal{E}}_0$ is the amplitude of the wave, z is the direction of propagation, k is the wave vector, and ω is the angular frequency. The wave vector k is given by

$$k = \frac{2\pi}{\lambda} = \frac{\omega}{v} = \frac{n\omega}{c}\,, \tag{A.33}$$

The use of complex solutions of the type given in Eq. A.32 simplifies the mathematics and is used extensively throughout this book. Physically measurable quantities are obtained by taking the real part of the complex wave.

where λ is the wavelength inside the medium. The first equality is the definition of k, the second follows by substitution of eqn A.32 into eqn A.25 with v given by eqn A.27, and the third follows from the definition of n given in eqn A.30.

The energy flow in an electromagnetic wave can be calculated from the **Poynting vector**:

$$\mathbf{I} = \boldsymbol{\mathcal{E}} \wedge \mathbf{H}\,. \tag{A.34}$$

This gives the power flow per unit area in W m^{-2}, which is equal to the **intensity** of the light wave. The intensity is defined as the energy crossing a unit area in unit time, and is therefore given by:

$$I = v u_\nu\,, \tag{A.35}$$

where v is the velocity of the wave and u_ν is the energy density per unit volume of the beam.

The Poynting vector given by eqn A.34 can be evaluated easily for the case of plane waves. Consider a wave polarized along the x axis of angular frequency ω propagating in the z direction. From eqn A.21 or A.22 we see that the magnetic field is perpendicular to the electric field. $\boldsymbol{\mathcal{E}}$ and $\mathbf{H}$ therefore form a right handed system as depicted in Fig. A.1. Hence the components of the wave must satisfy:

$$\begin{aligned}
\mathcal{E}_x(z, t) &= \mathcal{E}_{x0} \, \mathrm{e}^{i(kz - \omega t)} \\
\mathcal{E}_y(z, t) &= 0 \\
H_x(z, t) &= 0 \\
H_y(z, t) &= H_{y0} \, \mathrm{e}^{i(kz - \omega t)}\,.
\end{aligned} \tag{A.36}$$

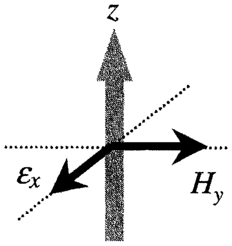

Fig. A.1 The electric and magnetic fields of an electromagnetic wave form a right handed system. The figure shows the directions of the fields in a wave polarized along the x axis and propagating in the z direction.

On substituting these fields into eqn A.21, we find that:

$$k\,\mathcal{E}_{x0} = \mu_o \mu_r \omega\, H_{y0}\,, \tag{A.37}$$

and hence that

$$H_{y0} = \frac{\mathcal{E}_{x0}}{Z} \tag{A.38}$$

where

$$Z = \frac{k}{\mu_0 \mu_r \omega} = \sqrt{\frac{\mu_0 \mu_r}{\epsilon_0 \epsilon_r}} = \frac{1}{c\epsilon_0 n}\,. \tag{A.39}$$

The second equality in eqn A.39 follows from eqns A.33 and A.27, while the third follows from Eq. A.28 and A.31 with $\mu_r = 1$. The quantity Z is called the **wave impedance**. On substituting eqns A.36–A.39 into eqn A.34, we obtain:

Z has a value of 377 Ω in free space.

$$I = \frac{\langle \mathcal{E}(t)^2 \rangle_{\text{rms}}}{Z} = \tfrac{1}{2} c\epsilon_0 n \mathcal{E}_0^2 \tag{A.40}$$

where $\langle \mathcal{E}(t)^2 \rangle_{\text{rms}}$ represents the root-mean-square time average. This shows that the intensity of a light wave is proportional to the square of the amplitude of the electric field. The relationship can be generalized for all light waves irrespective of the particular polarization of the beam.

In many topics covered in this book, it will be necessary to treat the refractive index as a complex number. A well-known example of how such a situation arises occurs when treating the propagation of electromagnetic waves through a conducting medium such as a metal. In a conductor, the current density is related to the electric field through the electrical conductivity σ according to:

$$\mathbf{j} = \sigma \boldsymbol{\mathcal{E}}\,. \tag{A.41}$$

Using this relationship to substitute for **j** in eqn A.13, and eliminating **D**, **B** and **H** in the same way that led to eqn A.25, we obtain:

$$\nabla^2 \boldsymbol{\mathcal{E}} = \sigma \mu_0 \mu_r \frac{\partial \boldsymbol{\mathcal{E}}}{\partial t} + \mu_0 \mu_r \epsilon_0 \epsilon_r \frac{\partial^2 \boldsymbol{\mathcal{E}}}{\partial t^2}\,. \tag{A.42}$$

We now look for plane wave solutions of the type given by eqn A.32. Substitution of eqn A.32 into eqn A.42 gives:

$$k^2 = i\sigma \mu_0 \mu_r \omega + \mu_0 \mu_r \epsilon_0 \epsilon_r \omega^2\,. \tag{A.43}$$

This can be made compatible with the usual relationship between ω and k given in eqn A.33 by allowing n to be a complex number. The complex refractive index is usually written $\tilde{n}$, and is defined by

$$k = \tilde{n} \frac{\omega}{c}\,. \tag{A.44}$$

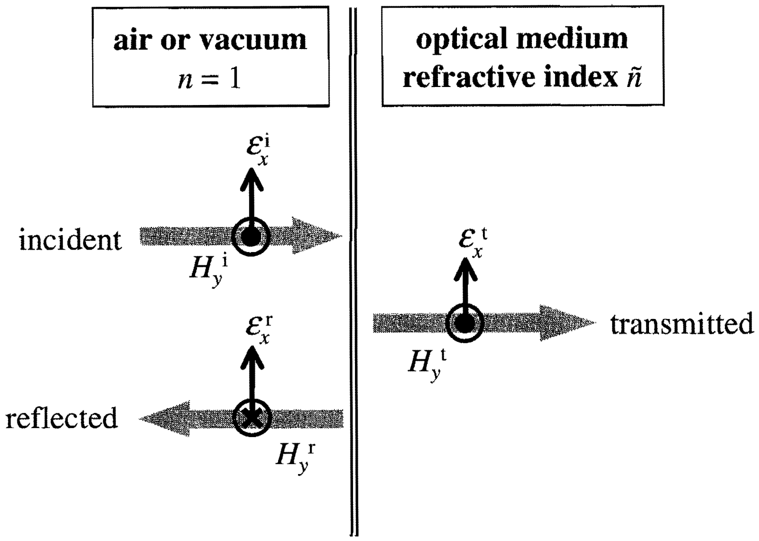

Fig. A.2 Transmission and reflection of light at an interface between air and a medium of refractive index $\tilde{n}$. The incident, transmitted and reflected rays are shown displaced from each other for clarity. All rays are normal to the interface. The symbol ⊙ for the magnetic fields of the incident and transmitted rays indicates that the field direction is out of the page, while the symbol ⊗ for the reflected wave indicates that the field is pointing in to the page.

By combining eqns A.43 and A.44 we obtain:

$$\tilde{n}^2 = \frac{\mu_r \sigma}{\epsilon_0 \omega} i + \mu_r \epsilon_r, \tag{A.45}$$

where we have made use of eqn A.28. This of course reduces to eqn A.31 if we set $\sigma = 0$ and $\mu_r = 1$. The physical significance of the complex refractive index implied by eqn A.45 is developed in more detail in Section 1.3.

It is shown in Chapter 7 that eqn A.45 is only valid at low frequencies. This is because the AC conductivity at high frequencies is not the same as the DC conductivity that enters eqn A.41.

The Maxwell equations also allow us to treat the transmission and reflection of light at an interface between two materials. This situation is depicted in Fig. A.2. Part of the beam is transmitted into the medium and the rest is reflected. The solution for an arbitrary angle of incidence was treated by Fresnel, and the resulting formulæ are known as **Fresnel's equations**. We restrict ourselves here to the simpler case when the angle of incidence is zero: that is, normal incidence.

We consider again an x-polarized light beam propagating in the z direction, with the field directions as shown in Fig. A.1. The electric and magnetic fields are given by eqn A.36. The beam is incident on a medium with complex refractive index $\tilde{n}$. The fields are related to each other through eqn A.38, with Z given by eqn A.39, although we now have to allow for the possibility that n may be complex.

The boundary conditions at the interface between two dielectrics tell us that the tangential components of the electric and magnetic fields are continuous. Applying this to the situation shown in Fig. A.2, we must have that both $\mathcal{E}_x$ and H_y are conserved across the boundary. Hence we can write:

$$\mathcal{E}_x^i + \mathcal{E}_x^r = \mathcal{E}_x^t, \tag{A.46}$$

and

$$H_y^i - H_y^r = H_y^t, \tag{A.47}$$

where the superscripts i, r and t refer to the incident, reflected and transmitted beams respectively. By making use of the relationship between the magnetic and electric fields given in eqns A.38–A.39, we can rewrite eqn A.47 as:

$$\mathcal{E}_x^i - \mathcal{E}_x^r = \tilde{n}\mathcal{E}_x^t, \tag{A.48}$$

where we have assumed that the light is incident from air with $\tilde{n} = 1$ and that $\mu_r = 1$ at the optical frequencies of interest here. Equations A.46 and A.48 can be solved together to obtain

$$\frac{\mathcal{E}_x^r}{\mathcal{E}_x^i} = \frac{\tilde{n} - 1}{\tilde{n} + 1}. \tag{A.49}$$

This can be rearranged to obtain the required result for the reflectivity R:

$$R = \left|\frac{\mathcal{E}_x^r}{\mathcal{E}_x^i}\right|^2 = \left|\frac{\tilde{n} - 1}{\tilde{n} + 1}\right|^2. \tag{A.50}$$

This formula is used in many examples throughout the book.

Further reading

The subject matter of this appendix is standard electromagnetism, and there are numerous books on the market that cover the material, for example: Bleaney and Bleaney (1976), Duffin (1990), Good (1999), Grant and Phillips (1990), Lorrain, Corson and Lorrain (1988). The subject is also covered in many optics text books such as Hecht (1998) or Born and Wolf (1999).